Journal Pre-proof

Computing resilience of process plants under Na-Tech events: Methodology and application to sesmic loading scenarios

Antonio C. Caputo , Bledar Kalemi , Fabrizio Paolacci ,
Daniele Corritore

PII: S0951-8320(18)31573-4
DOI: https://doi.org/10.1016/j.ress.2019.106685
Reference: RESS 106685

To appear in: *Reliability Engineering and System Safety*

Highlights

- A novel procedure for resilience calculation of process plants under Na-Tech events is proposed
- The methodology is strongly based on PERT/CPM technique and provides a direct estimation of capacity loss and the recovery time.
- The model can be applied both in deterministic and probabilistic manner and is generalizable to any kind of Na-Tech hazard
- The reliability of the methodology has been shown in computating the seismic resilience of an acid nitric plant

COMPUTING RESILIENCE OF PROCESS PLANTS UNDER NA-TECH EVENTS: METHODOLOGY AND APPLICATION TO SESMIC LOADING SCENARIOS

Antonio C. Caputo
Roma Tre University
Roma, Italy

Bledar Kalemi
Roma Tre University
Roma, Italy

Fabrizio Paolacci
Roma Tre University
Roma, Italy

Daniele Corritore
Roma Tre University
Roma, Italy

ABSTRACT

Resilience is a performance measure representing both the capability of a system to survive a disruptive event and the ability of rapidly restoring the operational status recovering the initial capacity. However, literature is lacking about methods allowing to compute resilience of process plants from a technical point of view. In fact, in the process industry the scarce literature about resilience mainly focused on organizational issues. In order to contribute to fill this gap a methodology has been developed to estimate resilience in case of Na-Tech events for process plants. The methodology provides a direct estimation of capacity loss after the disruptive event, and the time trend of recovery as well as the related economic loss. The model can be applied both in deterministic and probabilistic manner and is generalizable to any kind of Na-Tech hazard. However, in this paper specific reference is made to seismic hazard. In order to show the capabilities of the methodology a case study is also described referring to a Nitric Acid plant. Results show the predictive capabilities of this approach and the usefulness as a decision making tool for facility planners and emergency managers in the process industry.

KEYWORDS: Process plants; Resilience; Na-tech hazard; Seismic risk; Earthquakes.

NOMENCLATURE

A_{in} = Activity that corresponds to *n-th* reconstruction task related to *i-th* equipment;
BI = Business interruption cost;
β = Logarithmic standard deviation of the capacity distribution;
CBD = Capacity Block Diagram;
C_f = Normalized capacity of *f-th* process flow, $\in [0, 1]$;
$C_f(t)$ = Capacity of *f-th* process flow at time t;
Cn_f = Nominal production output of the *f-th* process flow;
$C_{s,f}$ = Normalized capacity of s-th stage of *f-th* process flow;
Cvu_f = Variable unit production cost of the *f-th* process flow;
$C(t)$ = Plant operational capacity at time t;
$DLS_{i,l}$ = Correspond to *l-th* damage limit state of *i-th* equipment;
DSB = Diamond shape buckling;
δ_i = State variable of *i-th* equipment;
Δt_z = Duration of the *z-th* time interval between functional recovery of two successive units;
EF = Earliest finish date of the generic activity;
EFB = Elephant foot buckling;
EL = Economic loss;
ER = Equipment reconstruction cost;
ES = Earliest start date of generic activity;
f = Annual probability of occurrence of a given seismic damage scenario;
f_{FA} = Mean annual frequency of failure of equipment;
f_{PGA} = Mean Annual frequency of exceeding a given PGA;
f_S = Mean annual frequency of survival of equipment;
F = Number of output process flows;

h(x) = Sampling distribution function of a variable;
$I_i(d)$ = Indicator function of event *I* for a damage *d*;
IS = Importance sampling technique;
LS = Latest start date of the generic activity;
LF = Latest finish date of the generic activity;
μ = The mean value of the capacity distribution;
M = Earthquake magnitude;
MCS = Monte Carlo Simulation;
N = Number of equipment in the plant;
N_{TOT} = Total number of combination of possible **SV**;
N_S = Number of simulations;
$N_{SV(K)}$ = Number of possible SV derived from all combination of *K* damaged units out of *N*;
O_f = Fraction of total plant capacity allocated to the *f-th* PF, $\in$ [0, 1];
ORAN = Overall Reconstruction Activities Network;
p_f = Unit selling price of the *f-th* process flow;
P_F = Probability of failure of equipment;
P_S = Probability of survival of equipment;
P_{THS} = Threshold value of scenario probability of occurrence or equipment probability of failure;
PF = Physical output material flow;
PFD = Process Flow Diagram;
PGA = Peak Ground Acceleration;
PS = Process stage;
PSHA = Probabilistic Seismic Hazard Analysis;
p(x) = Actual distribution function of a variable;
R = Distance of the site from the epicenter;
R_c = Overall residual plant capacity;
RC_{ij} = Cost of *j-th* restoration task required to recover functional status of the *i-th* equipment;
S_f = Number of sequential process stages of *f-th* process flow;
S [f] = Set of equipment used by the *f-th* process flow;
S [f,s] = Set of equipment used by the *f-th* process flow at the *s-th* stage;
$S_{K'}$ = Set of damaged units;
$S_{K''}$ = Set of undamaged units;
SL_k = Is the slack in time for each *k-th* activity;
SZ = Seismogenic zone;
SV = { δ_1, ..., δ_N} scenario vector;
t_0 = Time when disruptive event occurs;
t_a = Time when restoration activities start;
t_c = Time when recovery (increase) of plant capacity starts;
t_d = Time when damage propagation ends;
t_h = Control time usually defined by owners or decision makers;
t_r = Time when plant is fully restored;
T_{ij} = Duration of the *j-th* restoration task required to recover functional status of the *i-th* equipment;
T_{CRi} = Recovery date of the *i-th* unit;
TR = Recovery interval;
Φ = The standard Gaussian cumulative distribution;
w_M = Weight of magnitude used in IS;
w_R = Weight of distance used in IS;
w_{SZ} = Weight of seismogenic zone used in IS;
x = Number of operational units with fractionated capacity, connected in parallel;
z = Identifier of time interval between functional recovery of two successive units;
Z = Random number uniformly distributed in the range [0-1];

1. INTRODUCTION

Resilience is a concept which has attracted a great deal of interest from both public managers, industrial actors and the research community for over a decade. Although resilience is a wide ranging concept, which has been applied in many diverse contexts ranging from psychology, to metallurgy to organizational research, from the technical and managerial perspective it can be generally considered as a performance measure combining both the robustness of a system, intended as the ability to survive unexpected events which are able to disrupt its operations, and the capability of rapidly restoring system capacity after the disruptive event has occurred.

However, research aimed at assessing systems resilience in the last decade focused more on the civil infrastructures and building sector, as compared to the industrial one, and especially on networked systems, such as roads and transportation networks, supply chains, or service distribution infrastructures like gas and electricity distribution grids and telecommunication networks. Research on resilience of process plants and industrial facilities in general has been, instead, comparatively scarce, and mainly focused on organizational problems rather than aimed at providing a quantitative estimation model. Nevertheless, industrial facilities, and process plants in particular, that involve huge capital investments, may be a source of major accidents, thus representing a risk to nearby communities, contribute significantly to economic development of nations, and their failure can have a disruptive potential for global supply chains. Therefore, being able to assess plant resilience in case of disruptive events is inherently relevant, as local government, emergency responders, and business owners are interested in assessing the capability of the facility to withstand disruptive events and to rapidly return to normal operation. Moreover, knowledge of plant resilience allows to better plan protective and preventive measures, and is a building block to assess resilience of industrial supply chains.

Among the disruptive events which industrial plant face, natural hazards, like floods, hurricanes, tsunamis, earthquakes etc.., represent significant threats owing to their destructive potential. In industrial plants such natural hazard can give rise to Natural-Technological (Na-Tech) accidents which can have devastating consequences including equipment damage, release of dangerous substances, disruption of services and infrastructures, fatalities and environmental pollution with huge economic losses [1-3]. Research on seismic hazards in the process industry is a relevant topic and has been reviewed recently [4, 5]. Several models for quantitative risk assessment have been also made available [6-12]. Nevertheless, the above models focus on estimating equipment damage and losses consequent to the occurrence of an earthquake, but neglect the analysis of the capacity recovery process and plant resilience in general.

Resilience is a wide scope concept and performance measure, blending both the capability of a system to survive and the ability of rapidly recovering from high impact and low frequency disruptive events. This can be achieved by a mix of robust system design practices, damage prevention measures, organizational redesign as well as rapid recovery and survivability enhancing activities. Given its omnicomprehensive reach and applicability a single agreed definition of resilience has not yet been established. Therefore, several alternative definitions are discussed in the literature [13-15].

Generic overviews of the resilience concept in business and engineering contexts are provided by Hollnagel et al. [16] and Sheffi [17], while a general qualitative modeling framework has been also suggested by Rigaud and Guarnieri [18] and by Lundberg and Johansson [19]. Given the multiplicity of possible resilience definitions a wide range of quantitative performance measures and specific resilience metrics have been also proposed in the literature [14, 20, 21, 22, 23, 24].

From the management point of view resilience has been extensively studied under the organizational perspective [25, 26], as well as in the framework of enterprise management [27-31], including the economic impact on the social community [32] and the single business [33]. Input-output models have been also used to investigate the economic impact of natural or man-made hazards in industrial complexes and business sectors. However, the fields which attracted the major attention of researchers are those of civil and infrastructures engineering, networked infrastructures and supply chains.

In the field of civil engineering and built and transportation infrastructures, attention has been also focused on modeling resilience related to natural hazards. In particular, [34-37] review resilience modeling of built infrastructures under natural disasters conditions, and especially earthquakes [38-42]. Resilience of community structures in networks has been modeled by Ramirez-Marquez et al. [43]. Economic loss following natural disaster in urban communities and at regional level is also investigated by [44,45], while Barabadi and Ayele [46] attempt to use statistical analysis of historical data to estimate infrastructure recovery rates and time and Barker and Baroud [47] apply proportional hazard models to infrastructure recovery.

Networked and critical infrastructures, such as electricity grids or other utilities distribution networks, as well as computer networks also attracted a great deal of academic research. In this realm, apart from vulnerability to natural hazards, a major concern are cascading effects and external attacks either in stand-alone or interdependent networks [48-54]. This research also is aimed at resilience based network design [55] and identifying components importance in networks [56].

Networked systems include supply chains, which is another research field rising increasing interest, strictly related to networks and transportation systems resilience although with specific features [57-60].

Resilience research applied to industrial plants, instead, has been comparatively scarce even if such facilities are quite complex in itself, represent high capital investments and relevant cash flow streams for either the owner and other stakeholder, and a failure can have long duration effect which can propagate along the supply chains. In this sector, research has been mainly oriented towards the organizational and operational issues including human factors [61-64] and more recently to applications in safety analysis and risk assessment of process plants [65-69]. Ryzdak and coworkers [70-71] also attempted to model resilience using the system dynamics paradigm. Nevertheless, resilience modeling approaches derived from the networked infrastructures sector and from the civil and seismic engineering domain, may not be directly transferable to the field of industrial facilities, where resilience depends on fragility of process equipment and process flow structure. Ganesan and Elamvazuthi [72] develop a method for preliminary design process plants in order to optimize reliability, resilience and cost but using simplified process modeling and neglecting natural hazards. Tan et al. [73] develop a simplified model for an industrial plant based on process flow, but mainly from an economic perspective, and neglect disruptions from natural hazards. Zio and Ferrario [74], Ferrario and Zio [75, 76] investigate with detailed modeling safety-critical facilities, such as nuclear power plants subject to natural hazards. Nevertheless, in such kind of application product flow is not relevant, so that the approach cannot be directly applied to process plants as the emphasis is placed on the logical interactions of cascading effects on safety components and the affected processes. Mebarki et al. [77] deal with process plants but focus specifically on resilience of single process equipment under natural hazards thus neglecting the overall process flows. Finally, research is scarce too in the domain of manufacturing plants, although some general purpose modeling approaches have been suggested [70, 71, 78].

From the above discussion it appears that additional modeling effort, specifically targeted to process and manufacturing plants is still needed in order to obtain realistic resilience estimation of such facilities taking account their internal structures, the process flows and, in case of natural hazards, the inherent fragility of equipment.

In order to contribute to a solution of this research problem, in this paper an approach and associated software tool for the computation of process plant resilience, based on the actual process flows and installed equipment, is developed building on the preliminary work by Caputo and Paolacci [79]. The method has a general formulation and can be applied to any kind of disruption causing physical damage to plant equipment. It will be described with specific reference to earthquakes, even if it can be extended to any kind of Na-Tech event. Moreover, it can be applied both in a deterministic and probabilistic manner as described in the following. The method has the following notable features: it directly computes initial capacity loss after the disruption occurs; it computes the time trend of capacity recover and total recovery time; it estimates the total economic loss imputable to business interruption and plant reconstruction. In doing so, this model, while filling the above cited gap in the literature, may prove valuable as a decision making support tool for facility planning and emergency management in process industries.

This paper is organized in the following manner. A preliminary literature review discusses recent advances in resilience definition and quantification with special emphasis on the industrial sector. Subsequently the proposed algorithm for resilience computation is described assuming both deterministic and probabilistic scenarios and a generic disrupting event, with specific extensions to seismic risk. A case study application is successively described in order to show model capabilities with reference to a Nitric Acid Plant. Finally, model discussion and perspectives for future research conclude the paper.

2. MODEL DESCRIPTION

The model for resilience assessment is amenable to both a deterministic and probabilistic analysis. Deterministic resilience analysis implies that the user is interested in analyzing a specific damage scenario, meaning that the set of plant equipment damaged by the natural event, i.e. assigned to an out of service state, is predefined by the user. Any different damage scenario of interest can be separately analyzed. Probabilistic analysis implies that either the initial damage scenario is randomly generated, or that multiple possible damage scenarios are analyzed accounting for their probability of occurrence so that a probability distribution of the parameters of interest can be obtained. Finally, randomness can be included not only in the scenario generation but even in computing the duration of the recovery process. In this paper, although the deterministic approach will be mainly referred to for the sake of clarity, extension to probabilistic setting will be discussed when appropriate.

The method is aimed at computing the time trend of system capacity starting from the initial disruption up to the final recovery, as shown in schematic manner in Figure 1. Capacity, is considered here as the capability of generating a physical production output, intended to be the desired function of the system. Generally speaking, while the system operates at nominal capacity $C(t_0)$ let us imagine that a disruption caused by a natural event takes place at time t_0. The resulting equipment damage would impair the operational capacity which reaches a minimum residual value $C(t_d)$ at time t_d. Please note that capacity loss can be total, i.e. $C(t_d) = 0$, and that time interval (t_d-t_0) can be usually negligible for practical purposes. However, in case capacity loss is the consequence of damage propagation caused by cascading effects, it can happen that $(t_d - t_0) > 0$. Afterward the initial capacity loss a latency period (t_a - t_d) would follow to allow damage recognition and planning of required actions to recover capacity. Owing to restoration activities started at time t_a, capacity is gradually recovered starting at a time t_c and becomes fully restored at time t_r, so that in Figure 1, t_h represents a control time usually defined by plant owners or decision makers [80]. In Figure 1 the time trend of capacity recovery during period ($t_r - t_c$) has been generically depicted as linear, but this restriction can be relaxed in order to gain generality. In fact, in the literature several alternative capacity recovery functions, expressed in analytical manner have been proposed, including lognormal, exponential and trigonometric [36, 40]. In this work, nevertheless, the time trend of capacity recovery is computed on the basis of plant configuration, actual equipment damage and the time-phased sequence of restoration activities, instead of assuming a predefined time history. However, once the $C(t)$ function is known resilience can be precisely computed.

In the literature several expressions have been, in fact, proposed to make a point estimate of resilience. For instance, Bruneau et al. [81] refer to a "resilience loss"

$$RL = \int_{t_0}^{t_h}[100\%\text{-}C(t)]dt \quad (1)$$

while, according to Bocchini and Frangopol [82] and to Cimellaro et al. [80] resilience is computed in dimensionless form as

$$R = \frac{1}{t_h - t_0} \int_{t_0}^{t_h} C(t)dt \quad (2)$$

Nevertheless, in this work we are not only interested in computing a single valued measure of resiliency, or to stick to a determined formula, but rather to determine the initial capacity loss, i.e. residual capacity $C(t_d)$, the capacity recovery function $C(t)$ for $t \in [t_d, t_r]$ and the recovery interval $TR=(t_r - t_a)$ as well as the involved Economic loss ($EL=ER+BI$) including the equipment reconstruction cost (ER), i.e. the sum of the cost to perform all recovery activities related to the damaged units, and the business interruption cost (BI). By knowing the $C(t)$ function, in fact, any preferred equation in the literature can be used to compute a resilience performance measure. In any case, resilience will increase the higher is the residual capacity and the shorter is the recovery interval and the latency period.

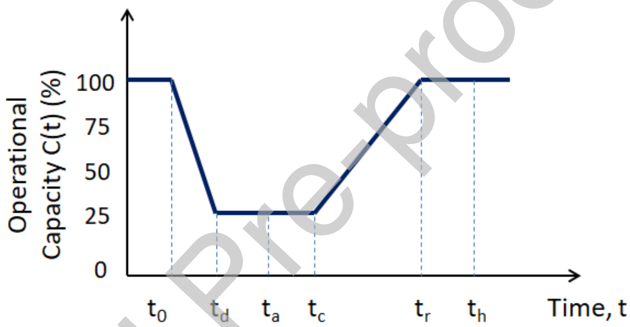

Figure 1 - Diagram of capacity vs time and characteristic times.

The proposed method includes 8 sequential steps, which are described in details as follows.

2.1. Process plant mapping

As a preliminary step the plant Process Flow Diagram (PFD) is inspected in order to identify the main equipment, the major piping connections, the relevant process streams and the associated utilities. In particular, all physical output material flows (PF) determining revenues, and the associated specific equipment involved in the corresponding sequence of processing operations of PFs, whose damage can impact the capacity of the process flow, are recognized. It is important to properly identify all material flows and equipment involved by each PF given that a PF may involve multiple process streams with equipment and process steps shared with other PFs. This analysis shall include utilities as well as main structural components. In fact, the failure of a utility can interrupt a process (i.e. the simple interruption of a cooling stream may bring a reactor which has not been physically damaged by an earthquake to a stop). In the same manner any structural item required for operating a process equipment, such as a pipe rack or a support structure, must identified and treated as an equipment as its failure can interrupt the process flow and will require a restoration activity. As a result a unique set **S[f]** of all process equipment, pipe lines and related structures pertaining to the *f-th* PF is thus defined, so that any damage to a unit included in **S[f]** may have an impact on the capacity C_f associated to that PF. In case the same equipment and utilities are shared by distinct PFs, they should be included in all the corresponding **S[f]**.

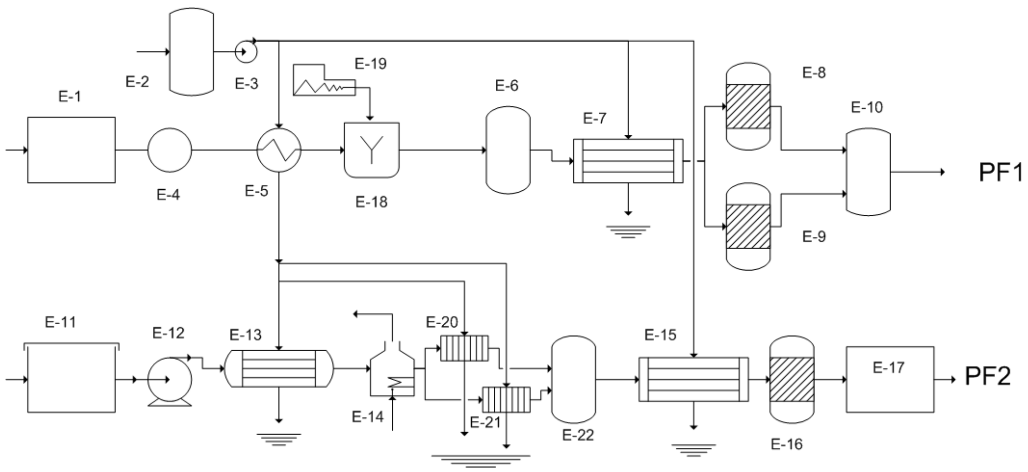

Figure 2 – Fictitious Process Flow Diagram.

In order to clarify this step let us consider the fictitious PFD of Figure 2 where process flows PF1 and PF2 can be identified. In this case **S[1]** = {E-1, E-2, E-3, E-4, E-5, E-6, E-7, E-8, E-9, E-10, E-18, E-19}, while **S[2]** = {E-2, E-3, E-5, E-11, E-12, E-13, E-14, E-15, E-16, E-17, E-20, E-21, E-22}, so that PF1 and PF2 share three equipment, namely E-2, E-3, and E-5.

2.2 Construction of process Capacity Block Diagram (CBD)

For each PF a Capacity Block Diagram (CBD) is drawn. In the CBD all equipment belonging to the corresponding set **S[f]**, are grouped in sequential process stages (PS) strictly connected in series. In this manner an equivalent representation of the PF is obtained as a series of PS, and the capacity of the PF becomes that of the PS having the lowest capacity, so that any capacity reduction occurring in the bottleneck PS would determine a corresponding capacity reduction in the whole PF. In case of total capacity loss within a PS then the overall PF is interrupted and total capacity loss of that process flow results. PSs do not necessarily correspond to physical process steps but rather to grouping of units which are arranged with the same logic from the process point of view. In this respect a PS can include a single or multiple units, and in the latter case it must include only units which are all arranged either in series or in parallel as far as the working logic of the process is concerned, as happens when building reliability block diagrams. Combination of series and parallel units in a single PS, is in general not allowed. When the PS includes units in series the entire stage capacity is lost when at least one unit is damaged. Conversely, in PS including units in parallel full capacity, partial capacity or zero capacity can result according to the number of failed units. In fact, in case of PS including parallel units it should be pointed out that a variety of parallel arrangements are possible according to the manner in which process is designed and equipment are sized and connected. Typical arrangements are:

i) pure parallel, where each redundant unit has enough capacity to handle the entire process flow so that PS capacity is lost when all units are failed, while at least one working equipment guarantees nominal capacity to that PS;
ii) fractionated capacity in parallel. In this case the PS capacity is equally subdivided in *n* parallel units and each unit can handle *1/n* of the entire process flow. Residual capacity is proportional to the number of surviving units, so that percent PS capacity is *x/n* when *x* units are operational.
iii) k-out-of n redundancy. In this case *n* equal units are installed in parallel but partial redundancy is obtained as full capacity is preserved only in case provided at least *k* units are operational, otherwise the PS capacity is lost.
iv) fractional parallel of unit in series. In this case one has *n* identical parallel branches of units in series. Each branch handles *1/n* of process flow but the branch capacity is preserved only in case all series units are operational.

v) parallel of series units. This is a fully redundant system composed of a parallel of n branches each including units in series. Full capacity is preserved when at least one parallel branch is operations (i.e. all its unit in series are operational).

For the sake of clarity, PFD of Figure 2 can be represented by two possible CBDs. Each CBD contains one PS with equipment in series and one PS with equipment in parallel with fractionated capacity. Respectively, (E-1, E-2, E-3, E-4, E-5, E-6, E-7, E-10, E-18, E-19) are equipment in series for PF1, while (E-2, E-3, E-4, E-11, E-12, E-13, E-14, E-15, E-16, E-17, E-22) are equipment in series for PF2. While the units E-8 and E-9 of PF1 as well as units E-20 and E-21 of PF2 are the one with fractionated capacity and each of them can handle half of the process stream.

2.3 Construction of Overall Reconstruction Activities Network (ORAN)

In this last preparatory step the activities required to restore functionality of possible damaged equipment and recover plant capacity, as well as the logical relationships between all such activities are represented as an acyclic oriented activity network. This will allow to compute the recovery date of each equipment and update production capacity estimation during the recovery period.

We must at first distinguish between common recovery activities and equipment-specific activities. For each *i-th* equipment or plant component included in **S[f]** vectors, the full list of activities to be carried out to restore its functionality is compiled at first. Equipment-specific activities may include foundations restoration, arranging contracts with suppliers, equipment repair or construction of a substitute one, transportation to plant site, on-site installation, fitting of insulation and auxiliary components such as sensors and instrumentation, painting, connection to utilities and to process stream piping, functional test, and so on.

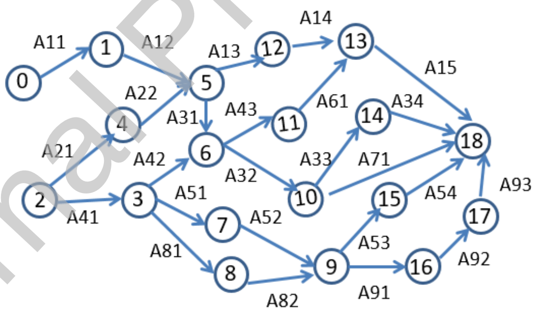

Figure 3 - Example of an Overall Reconstruction Activities Network (ORAN) for a plant including 9 units.

Common recovery activities instead may include preliminary recognition of damages, removal of failed equipment, site cleanup from spilled materials, clearance of access and internal roads, final plant commissioning and start-up etc. A duration T_{ij} has to be estimated for each *j-th* recovery task associated to the *i-th* equipment, resorting to empirical correlations, vendor information or the record of plant construction data. For each activity the list of all preceding tasks, which act as precedence constraints, has to be also compiled.

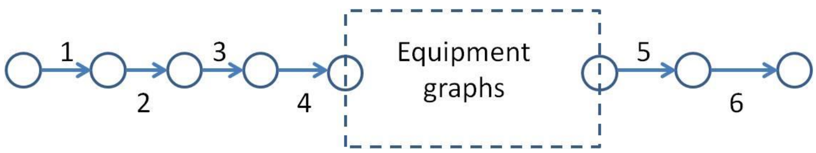

Figure 4 - Reference Overall Reconstruction Activities Network.

Legend: 1 = Emergency response, 2 = Access clearing, 3 = Site cleaning and remediation, 4 = Damage survey and recovery planning, 5 = Commissioning, 6 = Production ramp up.

(a)

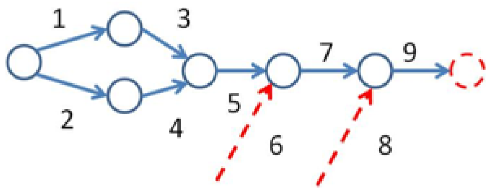

Legend: 1 = Dismantling and removal =, 2 = Specs definition and order, 3 = Foundation construction, 4 = Foundation construction, 5 = Installation, 6 = Connecting pipes installation, 7 = Piping connection, 8 = Electric plant installation, 9 = Electric connection.

(b)

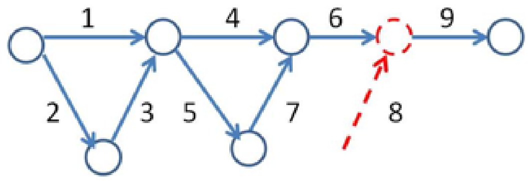

Legend: 1 = Dismantling and removal, 2 = Design, 3 = Materials delivery, 4 = Major electrical equipment installation, 5 = Installation of cables conduits and supports, 6 = Electrical connection, 7 = Cables laying, 8 = Equipment installation, 9 = Electrical connection to equipment, incl. switches and grounding.

(c)

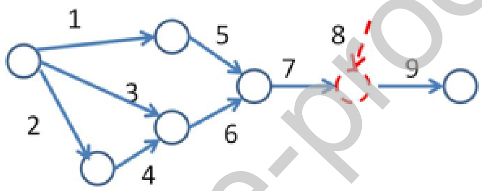

Legend: 1 = Design of piping system, 2 = Design of supports and rack, 3 = Dismantling and removal, 4 = Fabrication of supports and rack, 5 = Fabrication and delivery, 6 = Installation of supports and rack, 7 = Piping Installation, 8 = Equipment installation, 9 = Piping connection to equipment.

(d)

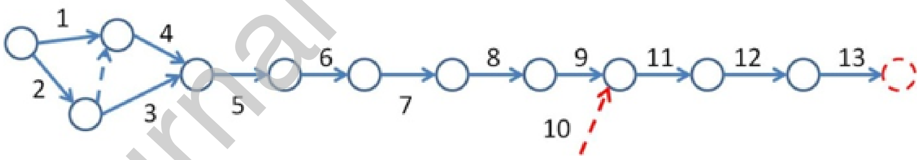

Legend: 1 = Removal of damaged equipment and site cleaning, 2 = Tank Design, 3 = Materials order and delivery (tank structure), 4 = Foundation construction, 5 = Base plates assembly, 6 = Walls assembly and internal fittings installation, 7 = Welding inspection, 8 = Roof building and installation, 9 = Ancillaries and fire-fighting equipment installation, 10 = Connecting pipes installation, 11 = Piping connection, 12 = Water filling and foundation settlement, 13 = Cleaning and testing, painting.

Figure 5 – Installation network of: a) Pump; b) Electrical distribution system network; c) Piping system; d) Vertical axis atmospheric storage tank.

It is important to identify precedence constraints between activities as this allows to define mutual interactions between restoration activities associated to distinct equipment. As an example it is true that an equipment cannot be installed until its foundation has been rebuilt, but after installation it cannot return into operational state until all necessary utilities are operational and pipe lines have been rebuilt and connected to the equipment, which cannot take place until reconstruction the structural supports for pipes has been completed.

After completing the global list of reconstruction activities for all plant equipment, including all precedence constraints among task, the plant reconstruction process shall be represented resorting to a network diagram, called ORAN (Overall Reconstruction Activities Network), similar to those widely used in project management practice known as PERT/CPM Technique [83]. An example of such a diagram, adopting the activity-on-arcs drawing convention, is shown in Figure 3 referring to a simple plant including 9 different equipment. Arrows in the network represent the reconstruction tasks, while nodes in the network represent start or finish event of the activities departing from or arriving to a node. Activity A_{in} corresponds to *n-th* reconstruction task related to *i-th* equipment. Completion of all activities converging into a node is required in order to start the activities departing from that node.

The generic architecture of an ORAN for a process plant is shown in Figure 4, where the graphs pertaining to each single equipment should be placed within the rectangle with dashed boundary line. Space limitations prevent from drawing a complete graph for a sample plant. However, single sample reference networks for relevant equipment types are shown in Figure 5, where dashed red arrows indicate interdependence with activities related to other equipment.

2.4 Damage scenario definition

2.4.1 Deterministic analysis

For a plant including N process equipment or main components, a vector **SV** = $\{\delta_1, \ldots. \delta_N\}$ can be defined, where a binary state variable δ_i is assigned to any *i-th* unit

$$\delta_i = \begin{cases} 0 & \text{if } i\text{-th equipment is damaged} \\ 1 & \text{if } i\text{-th equipment is not damaged} \end{cases} \tag{3}$$

At first **SV** is initialized setting $\delta_i=1, \forall i$.

In case of deterministic analysis the user selects a scenario to be investigated by deciding deterministically a list of equipment assumed to be damaged by the natural event. The initial damage scenario is then specified by setting to zero ($\delta_i=0$) the state variable for all damaged units thus determining the Scenario vector **SV**. By changing the initial **SV** setting any specific scenario of interest can be investigated. However, during the recovery period, switching from 0 to 1 the state variable of each damaged equipment as soon as it is taken back to operational status allows the **SV** to act as a State Vector used to represent the time-varying system status.

2.4.2 Probabilistic analysis

2.4.2.1 Scenario analysis

Instead of assuming the initial damage scenario in a deterministic manner, a probabilistic analysis can be carried out with reference to the uncertain damage that the natural event causes to the plant. This implies two distinct steps, namely the generation of damage scenarios and the computation of their probability of occurrence. A different capacity recovery curve will then result from each scenario.

The starting data to perform a probabilistic analysis is the hazard curve representing the mean annual frequency of exceeding a predefined level of the event intensity at the plant location for the considered natural hazard. Generation of hazard curves is a specific task beyond the scope of this work, so it is assumed as an input data. In the rest of this section reference will be made to seismic events but the approach can be easily generalized to other natural hazards.

In case of seismic hazard, provided that a seismic intensity measure has been chosen, for instance the Peak Ground Acceleration (PGA), the hazard curve specifies the mean annual frequency of exceeding a predefined intensity level of PGA at the plant location, based on site-specific geological conditions. The seismic hazard curve can be determined according for instance to the well-established Probabilistic Seismic Hazard Analysis (PSHA) approach introduced by Cornell [84].

It is assumed that in case of an earthquake, any *i-th* equipment can fail according to one or more failure modes associated to reaching a corresponding Damage Limit State (DLS). For instance, typical DLSs for unanchored vertical storage tanks include overturning, overtopping, sliding, buckling (i.e. Elephant Foot - EFB, Diamond Shaped - DSB); sloshing, floating roof damage, uplift, connecting pipes rupture, total equipment collapse [85]. Fragility curves can be used to estimate the probability of equipment failure $P_F(PGA)$ according to a predetermined DLS for a given value of the selected intensity measure. Equipment failure occurs when the seismic intensity is greater than equipment capacity which is assumed to behave as a random variable with log-normal distribution, so that [86]

$$P_F(PGA) = \Phi\left(\frac{1}{\beta} ln \frac{PGA}{\mu}\right) \tag{4}$$

where Φ is the standard Gaussian cumulative distribution, μ and β are respectively the mean value and logarithmic standard deviation of the capacity distribution. Fragility curves are available in the literature for a wide range of natural hazards, limit states and equipment types [87,88], otherwise they must be computed resorting to statistical analysis of damage data in historical Na-Tech events or by numerical modeling [89-92].

An alternative manner of expressing vulnerability functions is through Probit equations [6, 7, 86, 93, 94]. Probit value can be easy transformed into a failure probability P_F value [95].

Denoting f_{PGA} as the frequency of exceeding a given PGA, typically referred to a time of one year and provided by the seismic hazard curve, the corresponding mean annual frequency of failure of the equipment is

$$f_{FA,i,l}\left(PGA, DLS_{i,l}\right) = f_{PGA} P_{F,i,l}\left(DLS_{i,l}, PGA\right) \tag{5}$$

being $P_{F,i,l}\ (DLS_{i,l},\ PGA)$ the conditional probability of failure of the *i-th* equipment according to the corresponding fragility curve for the *l-th* DLS and a given PGA. However, given that an equipment is damaged when at least one limit state is reached (we assume independency of the DLS), the equipment probability to survive to the natural event with a given PGA is

$$P_{S,i}(PGA) = \prod_{l=1}^{DLS_i}\left(1 - P_{F,i,l}(PGA)\right) \tag{6}$$

and conversely $P_{F,i}(PGA) = 1 - P_{S,i}(PGA)$ is the equipment probability of failure. Meanwhile, the mean annual frequency that equipment survives a natural event with a PGA is $f_{S,i} = f_{PGA} P_{S,i}(PGA)$.

Once the failure probability of any equipment has been computed according to the specified intensity of the natural event, a damage scenario can be generated randomly, for instance resorting to Monte Carlo simulations, where a random number Z uniformly distributed in the range [0-1] is generated and compared with the equipment failure probability, so that when $Z \leq P_{F,i}$ the equipment is considered to be failed [8]. This random sampling is repeated for each equipment to determine the random scenario vector. Over n replications the relative frequency of a given SV is an estimate of its probability of occurrence.

Alternatively, the **SV** can be generated in an enumerative manner, as in the deterministic case, and for a given **SV** involving a specific set S_K' of K damaged units, and the complementary set S_K'' of (N-K) undamaged units, the probability of occurrence of that given **SV** is [10]

$$P(SV, PGA) = \prod_{i \epsilon S_{K'}} \left(1 - P_{S,i}\right) \prod_{j \epsilon S_{K''}} P_{S,j} \tag{7}$$

It should be noted that the number $N_{SV(K)}$ of possible **SV** deriving from all combination of K damaged units (Eq. 8 and 9), and the total number N_{TOT} of **SV** to be enumeratively analyzed grows very rapidly when N increases, so that the analysis can be limited only to those scenarios where the **SV** has a probability of occurrence higher than a user-defined threshold.

$$N_{SV(K)} = \binom{K}{N} = \frac{N!}{(N-K)!\,K!} \tag{8}$$

$$N_{TOT} = \prod_{K=1}^{N} \binom{K}{N} = 2^N - 1 \tag{9}$$

2.4.2.2 Risk analysis

A probabilistic seismic analysis of a process plant can be conducted according to the procedure proposed in [8], which is based on Monte Carlo Simulations. Consequently, the main starting damage scenarios (SV) and their rate of occurrence are determined, based on which resilience, economic losses and business interruption can be calculated.

The probabilistic seismic analysis starts with the identification of the seismically units damaged. For the *i-th* simulation, the Magnitude (*M*) of the seismic event and the Distance (*R*) of the site from the epicenter are randomly sampled. To improve the efficiency of the MCS, the importance sampling (IS) technique [96] is adopted. The magnitude and the distance are sampled from a uniform distribution between minimum and maximum value of the magnitude and the distance of the seismogenic zone from the site. Then, according to the IS, each event is weighted with a ratio $w=p(x)/h(x)$ between the actual distribution probability function $p(x)$ and the sampling distribution $h(x)$. So, different weights for the magnitude w_{Mi}, the distance w_{Ri} and the seismic activity of each region w_{SZi} are adopted to improve the convergence of the results.

The peak ground acceleration PGA_i is then determined by using seismic attenuation relationship and the corresponding probability of exceeding the DLS is established for each unit on the base of seismic fragility curves. According to the MCS, a random number Z (*0-1*) from a uniform distribution is generated for each unit and the *j-th* unit is considered damaged if:

$$Z < P_j(DLS|PGA_i) \tag{10}$$

where P_j is the probability of exceeding the DLS in the *j-th* unit, for $PGA=PGA_i$, deriving from the fragility curve. At the end of the simulations, the annual probability of occurrence of a given seismic damage scenario can be simply calculated as:

$$f = \sum_{i=1}^{N_S} \frac{I_i(d) w_{Ri} w_{Mi} w_{SZi}}{N_S} \tag{11}$$

where N_S is the number of simulations and $I_i(d)$ is the indicator function of the event i for a damage d.

2.5 Computation of initial capacity loss $C(t_d)$

Definition of the PF capacity block diagrams allows to compute in a straightforward manner the plant capacity according to the instantaneous value of the plant state vector. In fact the CBD may be used in a roughly similar manner to that in which a reliability block diagram is used to compute the so called Structure Function of a system allowing to assess whether the system is operational or not according to the status of its components.

In this step, **SV** and CBD are used at first to assess the initial capacity loss, i.e. residual capacity $C(t_d)$ as a percentage of nominal capacity. However, the same procedure can be applied to determine the subsequent time history of plant capacity during the recovery period by updating the SV according to the unit recovery.

Table 1 - Stage capacity computational models.

PS with units in series (*i* is the generic *i-th* unit)	$C_{s,f}= \prod_{i\in S[f,s]} \delta_i$
PS with multiple identical redundant units (*i* is the generic *i-th* unit)	$C_{s,f}= Max\{\delta_i\},\ i\in S[f,s]$
PS with identical multiple series subsystems in parallel (*i* is the generic *i-th* unit in the *j-th* parallel branch)	$C_{s,f}= Max_j \left\{\prod_i \delta_{i,j}\right\},\ i,j\in S[f,s]$
PS with capacity fractionated into n equal units in parallel (*i* is the generic *i-th* unit, n is the number of units located in PS)	$C_{s,f}= \sum_{i\in S[f,s]} \frac{1}{n} \delta_i$
PS with capacity fractionated into n identical subsystems of units in series (*i* is the generic *i-th* unit in the *j-th* branch, n is the number of subsystems branches allocated in PS)	$C_{s,f}= \sum_{j\in S[f,s]} \frac{\prod_i \delta_{i,j}}{n}$
PS with redundant *k* out of *n* equal units (*k* is the number of units that are needed to be operational in order to maintain the full capacity of *s-th* PS of *f-th* PF, while n is the number of units allocated in PS)	$C_{s,f}= \begin{cases} 1 \text{ if } \sum_{i\in S[f,s]} \delta_i \geq k \\ 0 \text{ if } \sum_{i\in S[f,s]} \delta_i < k \end{cases}$

Having defined sets **S[f]** and the CBD with the corresponding PS, the definition of sets **S[f,s]** including all equipment used by *the f-th* process flow at the *s-th* stage follows. As the PS are in series, the normalized capacity of the *f-th* process flow corresponds to the instantaneous capacity of the PS having the lower capacity, which will act as a bottleneck,

$$C_f = Min\{C_{s,f}\} \tag{12}$$

In Equation (12) $C_{s,f}$ is the normalized capacity of *s-th* stage of *f-th* process flow, and values of $C_{s,f}$ are computed as shown in Table 1 according to the kind of arrangement of the equipment included in each stage and the initial value of state variables as indicated by the state vector **SV**. Using formulas of Table 1 the value of $C_{s,f}$ is computed as a percentage of the nominal PS which, unless otherwise specified, is assumed equal to the absolute nominal capacity of the corresponding PF. This means that it is assumed that capacity is balanced among process stages, even if this constraint can be easily relaxed. In case of total capacity loss within a PS then the overall PF is interrupted and total capacity loss of that process follows.

For process stage configurations different from those listed in Table 1 specific expressions for computing stage capacity as a function of state variables should be developed on a case-specific basis. Finally, by summing over all PF the partial capacities one computes the overall residual plant capacity as:

$$R_c = \sum_f C_f O_f \tag{13}$$

where, O_f is the fraction of absolute total plant capacity allocated to the *f-th* PF.

2.6 Determination of Capacity recovery function C(t)

Equations (12), (13) and formulas of Table 1 allow to update PF and plant capacity as soon as each single units is taken back into service by switching its corresponding state variable δ_i from 0 to 1. Therefore, by keeping track of the status of each equipment during the recovery period, the time trend of the recovery function can be determined provided that the date of occurrence of state change for each process unit can be estimated.

This is readily accomplished resorting to the ORAN, as this allows to compute the finish date of equipment recovery tasks accounting for all task interdependence.

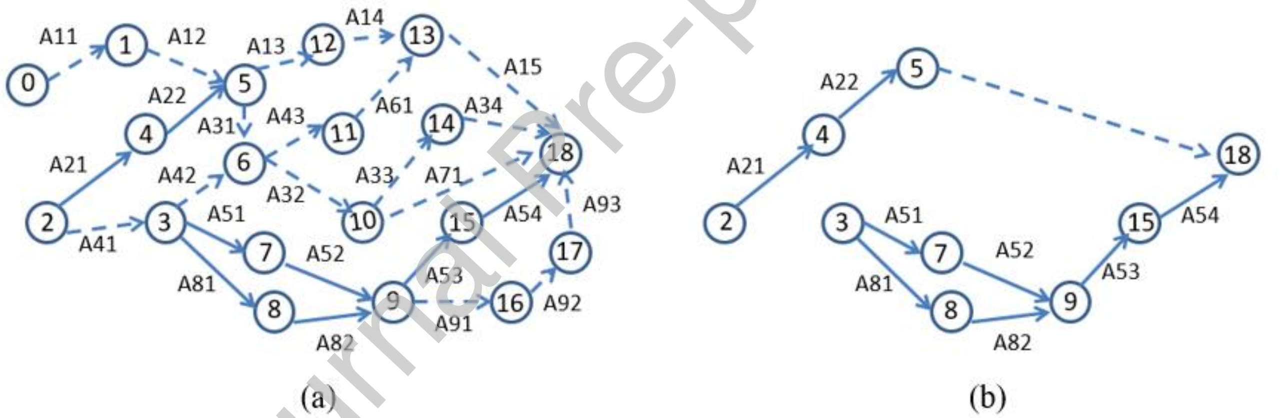

Figure 6 - a) ORAN showing activities with zero duration (dashed arrows) according to a sample scenario vector. b) Actual recovery activities network according to selected the scenario vector.

Nevertheless, it should be pointed out that the ORAN is a generic network including all possible recovery tasks, and is drawn only once for a given process plant, while the actual recovery activities to be carried out depend on the specific equipment to be restored as a consequence on the damage as specified by the assumed scenario vector. Changing the SV, the set of equipment to be restored changes along with the list of recovery activities to be carried out, thus changing the recovery function of the plant.

Therefore, in order to compute the actual recovery function, after defining **SV** and computing *C(t_d)*, the specific activity network corresponding to that **SV**, called the Scenario Network (SN) should be generated. It is not necessary to build a specific SN for each **SV**, as this can be directly obtained automatically by the ORAN by setting $T_{ij}=0$ for all units where $\delta_i = 1$ in the chosen SV. As an example Figure 6 shows the generation of the SN from the sample ORAN depicted in Figure 3 assuming for instance that the selected scenario included damage to units 2, 5, 8, while units 1, 3, 4, 6, 7 and 9 are undamaged, so that the duration of their recovery activities, shown in Figure 6 (a) with dashed lines, is set to zero.

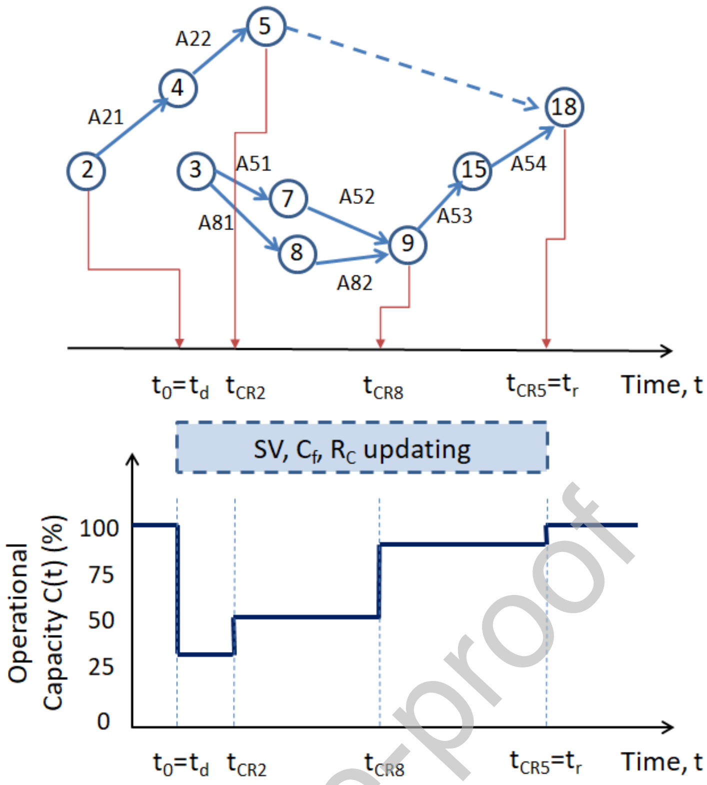

Figure 7 - Sample time trend of capacity recovery according to a given SV.

A schedule for activities completion and equipment recovery can be then computed resorting to traditional algorithms for activities network solution as described below.

In particular, starting from the first node (representing the start of the first activity) and proceeding towards the last node (representative of termination of the capacity recovery process) for each generic *l-th* activity the Earliest Start date (ES_l) is determined as $ES_l = Max\ (EF_k)$ with subscript k denoting all preceding activities whose arc terminates in the node from which the *l-th* activity departs. Once (ES_k) is computed, the Earliest Finish date (EF_k) of the generic *k-th* activity terminating in that node is $EF_k = ES_k + T_k$, being T_k the duration of the *k-th* task (corresponding to T_{ij} once a value of i and j has been defined). The ES date for the first activity can be assumed equal to t_d. In this manner an earliest occurrence date for the events represented by all nodes may be determined. The EF date of the final activity corresponds to the completion date of the capacity recovery process (i.e. value t_r), allowing to determine the duration of the recovery period (t_r - t_d). By proceeding backwards from the final node to the initial one it is possible to compute the Latest Finish date (LF_l) for the *l-th* activity $LF_l = Min\ (LS_k)$ once the Latest Start date (LS_k) has been computed for all *k-th* activities departing from the node where the *l-th* activity terminates, being $LS_k = LF_k - T_k$.

For each *k-th* activity the slack $SL_k = LS_k – ES_k$ can be computed. In case $SL_k = 0$ the activity is denoted as critical. The set of critical activities determine the critical path, whose duration corresponds to the duration of the recovery process. For non-critical activities the completion date is conventionally set as the average between the earliest and latest finish dates. A probability density function for the critical path duration can be also computed by assuming random activities duration, as happens in PERT method, but this is neglected here as for sake of simplicity. The above mentioned procedure is the same as the one in used in project management practice, known as PERT/CPM Technique [83].

The recovery date for each *i-th* damaged equipment, denoted T_{CRi}, is set equal to the completion date of the final recovery task related to that equipment. This allows to create a list of recovery dates for all damaged equipment, ordered for increasing T_{CRi} values. In order to compute the time trend of capacity recovery, at each time value $t = T_{CRi}$, the corresponding equipment state variable is set back to $\delta_i = 1$, the State Vector is updated, the PF capacity is updated through Eq. (12), and plant residual capacity is updated through Eq. (13). A graphical depiction of this procedure is shown in Figure 7.

2.7 Determination of economic loss

Economic loss ($EL = ER + BI$) caused by natural event includes the equipment reconstruction cost (ER), i.e. the sum of the cost to perform all recovery activities related to the damaged units, and the business interruption cost (BI) associated to lost production and quantified as the lost contribution margin of the affected process flows. The latter is to be computed separately for each PF and summed over all PF. No fatality cost is included in this model. *ER* and *BI* are computed as follows

$$ER = \sum_i \sum_j \delta_i \, RC_{ij} \tag{14}$$

$$BI = \sum_f \sum_z \left(p_f - Cvu_f\right)\left[Cn_f - C_f(t)\right]\Delta t_z \tag{15}$$

In Eq. (14) the term RC_{ij} is the cost of *j-th* restoration task required to recover functional status of the *i-th* equipment, and δ_i corresponds to the initial value included in the scenario vector, while in Eq. (15) $C_f(t)$ is the capacity of *f-th* process flow at time *t*, Cn_f the nominal production output of the *f-th* process flow, Cvu_f the variable unit production cost of the *f-th* process flow, p_f the unit selling price of the *f-th* process flow, and Δt_z the duration of the *z-th* time interval between functional recovery of two successive units.

In Eq. (14), summation over *z* allows to compute the *BI* cost over the entire duration of the capacity recovery period while keeping track of partial capacity recovery and the corresponding reduction of lost contribution margin as the production output is gradually restored.

The proposed model is implemented in Matlab and the entire algorithm is summarized in Figure 8. The algorithm is shown for the case of Na-Tech seismic event, but it can be used for any Na-Tech event, the only change will be in defining the damage scenario vector which is an input for resilience calculations.

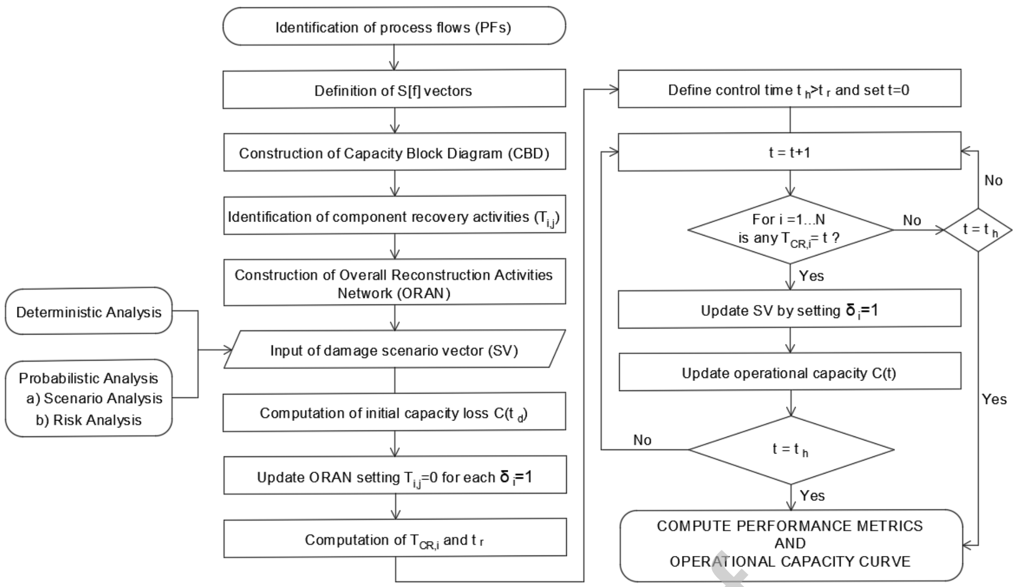

Figure 8 - Resilience computation algorithm in case of seismic Na-Tech event.

The above model can be used to determine the capacity recovery curve and economic losses for any predefined specific scenario. Otherwise the analysis can be repeated for multiple scenarios. Each damage scenario will be characterized by its distinct initial capacity loss and residual capacity $C(t_d)$, duration of recovery period (t_r-t_d), *ER* and *BI* values, and a corresponding probability of occurrence. A complete probabilistic analysis requires to analyze all possible damage scenarios, i.e. Scenario Vectors (SV) and seismic events. This requires generation of random scenarios or systematic enumeration of possible credible scenarios (i.e. possible values of SV vectors) as discussed in Section 4.2, the resilience assessment being carried out separately for each SV and each intensity level of the natural event according to the site hazard curve. A threshold value P_{THS} can be assigned to the scenario probability of occurrence or to the equipment failure probability, so that only equipment and scenarios having a probability greater than the cut-off threshold are evaluated. When multiple scenarios are analyzed, considering the probability of occurrence of each one, the corresponding capacity recovery histories can be generated and the probability distribution of all variables of interest describing plant resilience can be obtained, as shown schematically in Figure 9.

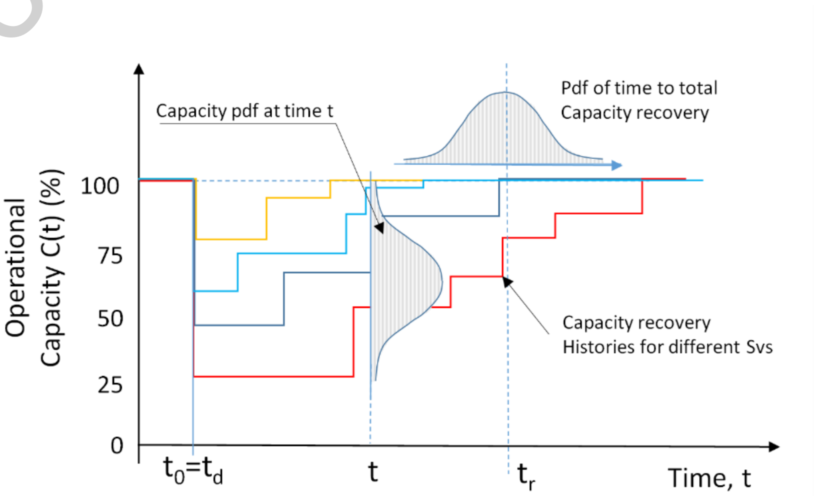

Figure 9 - Conceptual scheme of probabilistic resilience analysis.

3. APPLICATION TO NA-TECH EVENTS: EARTHQUAKE LOADING SCENARIO

In this section the proposed methodology is applied to a specific case study, the nitric acid plant described in Ray and Johnston [97], properly modified to include more complex conditions. After a brief description of the plant, the most frequent seismic damage scenarios are evaluated by using the methodology proposed by [8]. Finally, the resilience calculation and the business interruption evaluation for the analyzed example are described and commented, showing the full potentiality of method.

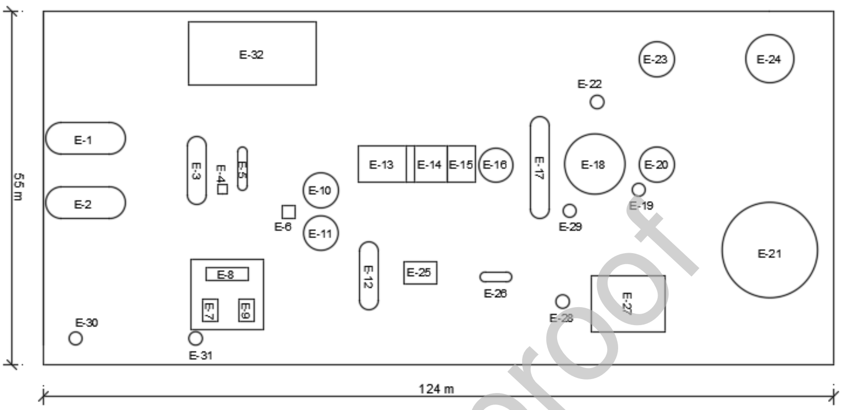

Figure 10 - Plant Plan View.

3.1 Description of case study

A nitric acid plant, with a plant view as shown in Figure 10, is selected as a case study for resilience calculation. Plant contains 32 equipment and 7 groups of pipes which make a total of 39 elements to be considered in calculation as per Table 2. The major equipment are ammonia storage tanks, ammonia vaporizer, ammonia filter, ammonia super-heater, two-stage air compressor, mixer, reactors, steam super-heater, waste-heat boiler, tail gas pre-heater, cooler/condenser, oxidation vessel, secondary cooler, liquid vapor separator, tail gas warmer, refrigeration unit, absorption column, pumps, bleaching columns, nitric steel storage tanks, electric unit and piping systems.

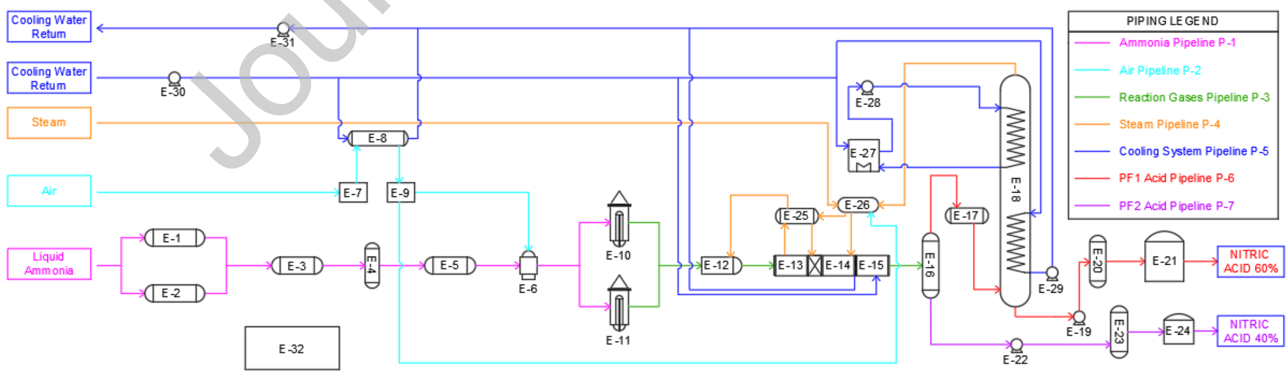

Figure 11 - Process Flow Diagram of nitric acid plant.

The plant has two Process Flows (PF), with 60% of total plant capacity allocated in PF1 and 40% of total plant capacity allocated in PF2. PF1 delivers 195 t/d of nitric acid (60% concentration), while PF2 delivers 130 t/d of nitric acid (40% concentration), based on 8000 hours of operation per year. The simplified process flow diagram of the plant is shown in Figure 11. Two sets of equipment are identified, **S[1]**={E-1, E-2, E-3, E-4, E-5, E-6, E-7, E-8, E-9, E-10, E-11, E-12, E-13, E-14, E-15, E-16, E-17, E-18, E-19, E-20, E-21, E-25, E-26, E-27, E-28, E-29, E-30, E-31, E-32, E-33, E-

34, E-35, E-36, E-37, E-38} and **S[2]**={ E-1, E-2, E-3, E-4, E-5, E-6, E-7, E-8, E-9, E-10, E-11, E-12, E-13, E-14, E-15, E-16, E-22, E-23, E-24, E-25, E-26, E-30, E-31, E-32, E-33, E-34, E-35, E-36, E-37, E-39}.

Purchase cost of equipment are indicated in Table 2 based on the work of Ray and Johnston [97], which refers to 1986. In order to calculate current cost of equipment the Chemical Engineering Plant Cost Index (CEPCI) [98] is used. The base index is 100 corresponding to 1957-59, while in 1986 it was 318.4 [99]. Consequently, the current cost of equipment's is calculated by using the index of 2018, which increased, from 1989, of around 88 % [98]. Accounting for the September 2018 exchange ratio of A$ to Euro (0.62), the current replacement costs of each equipment are indicated in Table 2.

Each PF is presented by 3 Capacity Block Diagrams (CBD), one with elements in series and two with capacity fractionated into 2 equal units in parallel, as shown in Figure 12. The piping systems are assembled in 7 groups and considered as elements in series, as the failure of one of them would interrupt the flow of the corresponding PS's.

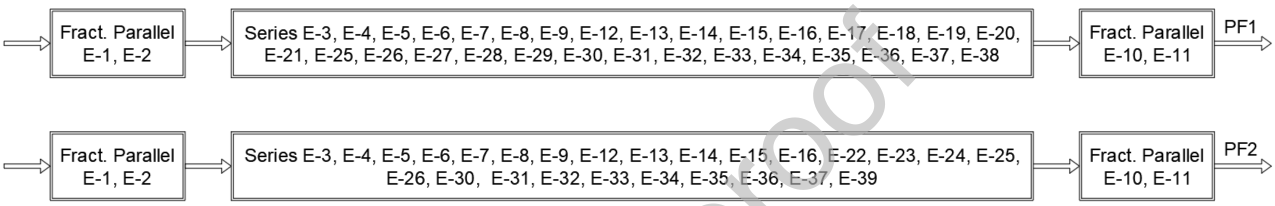

Figure 12 - Capacity Block Diagrams of Nitric Plant PFs.

Table 2 - Equipment replacement cost and seismic fragility parameters.

Eq. Label	Process Equipment	Replacement cost (€)	PGA_m (g)	β	Damage state	Reference
E-1	Ammonia storage vessel	646,000	0.54	0.46	PL2	Horizontal Vessel [*]
E-2	Ammonia storage vessel	646,000	0.54	0.46	PL2	Horizontal Vessel [*]
E-3	Ammonia Vaporizer	70,000	0.54	0.46	PL2	Horizontal Vessel [*]
E-4	Filter	30,000	1.00	0.60	DS3	Mechanical Equipment [**]
E-5	Ammonia Superheater	34,000	0.54	0.46	PL2	Horizontal Vessel [*]
E-6	Mixer	30,000	1.00	0.60	DS3	Mechanical Equipment [**]
E-7	1-st Stage Air Compressor	1,458,000	0.77	0.65	DS4	Compressor Station [**]
E-8	Compressor intercooler	61,000	0.54	0.46	DS4	Horizontal Vessel [*]
E-9	2-nd Stage Air Compressor	2,722,000	0.77	0.65	DS4	Compressor Station [**]
E-10	Reactor	139,000	0.51	0.45	PL2	Vertical Vessel CL1 [*]
E-11	Reactor	139,000	0.51	0.45	PL2	Vertical Vessel CL1 [*]
E-12	Steam Super-Heater	74,000	0.54	0.46	PL2	Horizontal Vessel [*]
E-13	Waste Heat Boiler	86,000	0.54	0.46	PL2	Horizontal Vessel [*]
E-14	Tail Gas Pre-heater	72,000	0.54	0.46	PL2	Horizontal Vessel [*]
E-15	Cooler/Condenser	186,000	0.54	0.46	PL2	Vertical Vessel CL1 [*]
E-16	Oxidation Vessel	101,000	0.59	0.41	PL2	Vertical Vessel CL2 [*]
E-17	Secondary Cooler	250,000	0.54	0.46	PL2	Horizontal Vessel [*]
E-18	Absorption Column	2,261,000	0.67	0.37	PL2	Extrapolation [*]
E-19	Acid Pump	10,000	1.60	0.60	DS4	Horizontal Pump [**]
E-20	Bleaching Column	74,000	0.59	0.41	PL2	Vertical Vessel CL2 [*]
E-21	Nitric Acid (60%) Tank	1,160,000	0.68	0.75	DS4	Unanchored Tank [**]
E-22	Acid Pump	10,000	1.60	0.60	DS4	Horizontal Pump [**]

E-23	Bleaching Column	74,000	0.59	0.41	PL2	Vertical Vessel CL2 [*]
E-24	Nitric Acid (40%) Tank	696,000	0.68	0.75	DS4	Unanchored Tank [**]
E-25	Liquid Vapor Separator	70,000	0.54	0.46	PL2	Horizontal Vessel [*]
E-26	Tail Gas Warmer	124,000	0.54	0.46	PL2	Horizontal Vessel [*]
E-27	Refrigeration Unit	164,000	1.00	0.60	DS3	Mechanical Equipment [**]
E-28	Water pump	3,000	1.25	0.60	DS4	Vertical Pump [**]
E-29	Water pump	3,000	1.25	0.60	DS4	Vertical Pump [**]
E-30	Water pump	3,000	1.25	0.60	DS4	Vertical Pump [**]
E-31	Water pump	3,000	1.25	0.60	DS4	Vertical Pump [**]
E-32	Electric Unit	811,000	1.00	0.80	DS3	Electric Power [**]
E-33	Ammonia Pipeline	541,000	1.00	0.60	DS5	Elevated Pipes [**]
E-34	Air Pipeline	541,000	1.00	0.60	DS5	Elevated Pipes [**]
E-35	Reaction Gas Pipeline	541,000	1.00	0.60	DS5	Elevated Pipes [**]
E-36	Steam Pipeline	541,000	1.00	0.60	DS5	Elevated Pipes [**]
E-37	Cooling System Pipeline	55,000	1.00	0.60	DS5	Elevated Pipes [**]
E-38	PF1 Acid Pipeline	541,000	1.00	0.60	DS5	Elevated Pipes [**]
E-39	PF2 Acid Pipeline	541,000	1.00	0.60	DS5	Elevated Pipes [**]

(PEC, 2017 [87]) [*], (Hazus MH 2.1 [88]) [**]

The total variable unit production cost of 1 t of 100 % nitric acid in 1986 was 97.07 A$, which corresponds to 59.30 A$ (36.8 €) for 1 t of 60 % nitric acid and 38.8 A$ (24.0 €) for 1 t of 40 % nitric acid [97]. Taking into account inflation, a variable unit production cost of 60 €/t and 40 €/t will be adopted respectively. The selling price of 100 % nitric acid in the world market in 1986 varied between 339 and 487 A$/t [97]. For our purpose, a value of 400 €/t, including inflation will be considered, which corresponds to a price of 240 €/t and 160 €/t for 60 % and 40 % nitric acid, respectively. The recovery times of equipment for any damage scenario are based on ORAN of plant as described in Section 3.3 and it has been implemented in Matlab environment. We assume that there is no limitation in working force, so repairing of all equipment's will start after finishing the pre-work activities: emergency response; access clearing; site cleaning and remediation, damage survey and recovery planning as shown in Figure 4.

3.2 Evaluation of the seismic damage scenarios

The nitric acid plant is supposed to be fictitiously placed in one of the most seismically active zones in Sicily (Italy), just closed to Priolo Gargallo city, and characterized by a soil type B.

In this case study the most probable damage scenarios will be defined using risk analysis as presented in section 3.4.2.2. The parameters for evaluation of the fragility curves are specified in Table 2, where the median value of ground motion PGA_m and the lognormal standard deviation β for each group of process equipment are selected from literature [87, 88] considering the units affected by an extensive damage.

The results of the probabilistic seismic analysis of the nitric acid plant are obtained with PRIAMUS software [100], a software developed in Matlab® environment that include the procedure previously depicted.

Table 3 - Initial seismic damage scenario probability.

#	Seismic damage scenario (damaged units)	Annual Probability
0	None	0.999
1	E-21 E-24	1.39e-06
2	E-32	9.05e-07
3	E-24	3.22e-07
4	E-21	2.63e-07
5	E-7 E-9	1.90e-07
6	E-10 E-11	9.93e-08
7	E-1 E-2 E-3 E-5 E-8 E-12 E-13 E-14 E-15 E-17 E-25 E-26	7.29e-08
8	E-9	7.05e-08
9	E-10	6.37e-08
10	E-11	4.77e-08
11	E-7	4.08e-08
12	E-1 E-2 E-5 E-12 E-25	2.71e-08
13	E-4 E-6 E-27 E-33 E-34 E-35 E-36 E-37 E-38 E-39	2.68e-08
14	E-16 E-20 E-23	2.02e-08
15	E-21 E-24 E-32	1.64e-08
16	E-2 E-3 E-5 E-8 E-13 E-14 E-15 E-17 E-25 E-26	1.55e-08
17	E-16	1.52e-08
18	E-24 E-32	1.35e-08
19	E-10 E-11 E-32	1.34e-08

Table 3 lists the most likely initial seismic damage scenarios along with the relevant annual probability of occurrence. It can be noticed that a seismic scenario with all undamaged equipment entails the higher probability of occurrence (0.999). A probability of 1.39 E-06, is associated to the contemporarily damaging of the tanks E-21 and E-24; these units represent the most vulnerable ones. In decreasing order, in fact, the damage of electric unit E-32 occurs with a probability of 9.05e-07. Scenarios with more than two damaged equipment are also possible; for example, the contemporarily damaging of the units E-1, E-2, E-3, E-5, E-8, E-12, E-13, E-14, E-15, E-17, E-25 and E-26 corresponds to a very low probability of occurrence of 7.29 E-0.8.

For completeness, Figure 13 shows for each equipment the individual annual probability of being seismically damaged. It can be noticed that according to the previous results, the tanks E-21 and E-24 are the equipment with the highest probability of damage ~1.80 e-06. This is not surprising, being storage tanks one of the most vulnerable elements of a plant [1, 94].

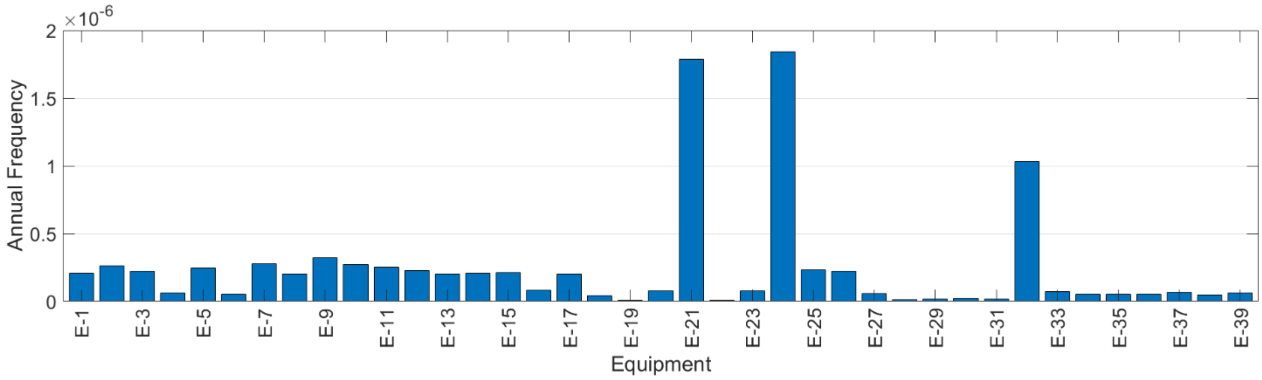

Figure 13 - Mean annual frequency of the seismic damage for the single equipment.

3.3 Resilience and business economic losses evaluation

In this section the resilience calculation for the single component and the influence of the seismic damage scenarios on resilience is presented. At this purpose a control time t_h*=180 d*, equal to the maximum duration of reconstruction of plant when all elements are damaged, is used in order to calculate the resilience of all units, which is based on Eq.(2), and shown in Figure 14. Acid pump of PF2 (E-23) is the most resilient element (91.3 %) while 60 % nitric acid storage tank (E-21) is the least resilient element (40 %). In addition, E-7, E-9 and E-32 are rather low resilient elements (less than 50 %); this is related both to a high recovery time and because they are elements in series used by both PFs.

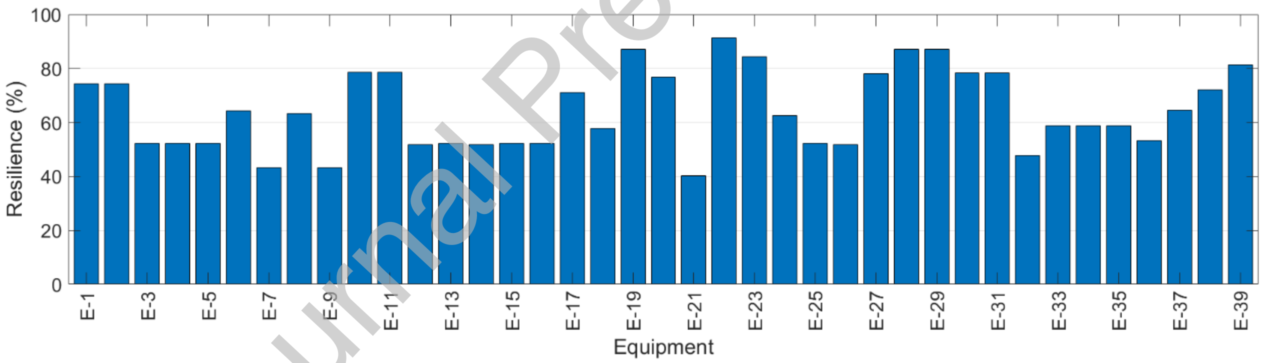

Figure 14 - Resilience of the single equipment.

Figure 15 shows the economic losses in case a single equipment is damaged. It can be noticed that the least resilient equipment (*R*=40 %), nitric acid 60 % storage tank (E-21) of PF1 (Figure 14), is the one which cause the biggest Business Interruption Loss as due to its longest time to be repaired, which is about 6.3 million euros, against a total economic loss of 7.4 million euros. The most resilient equipment, (*R*=91%), is the acid pump of PF2 (E-22), which has the smallest Business Interruption Losses (0.6 million euros) and a total loss of 0.62 million euros. The biggest economic loss is instead evidently caused by the failing of second stage compressor (E-9), which would cost the plant owner around 7.9 million euros.

The above information is very useful for plant owners, decision makers, facility planners, emergency managers and insurance companies. In particular, plant owners and decision makers can be guided in identifying the most critical equipment (e.g. the E-21) and proper mitigation strategies. Information about low-resilient equipment can also be useful to improve emergency or recovery plans. In addition, information about economic losses and business interruption effects can also be of interest for insurance companies.

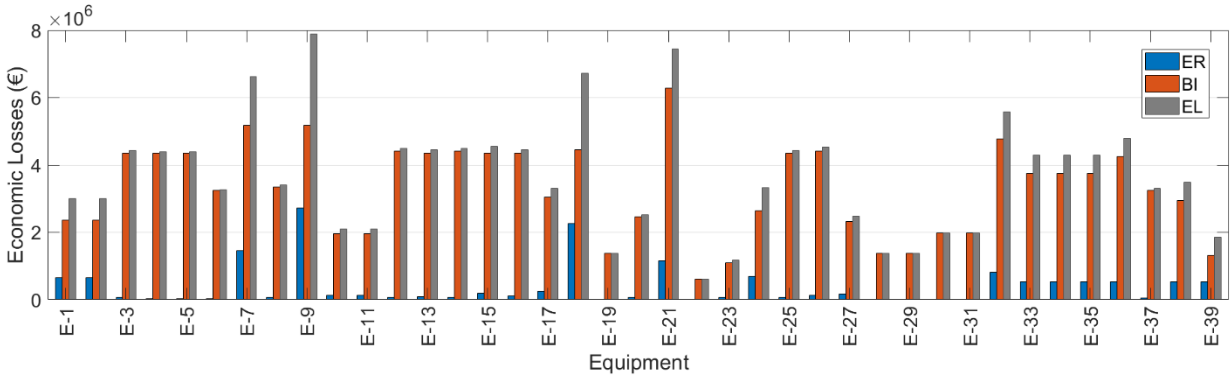

Figure 15 - Business economic losses in case of single element damaged.

Figure 16, shows the mean annual frequency of the most probable seismic damaged scenarios, while Figure 17 shows the related economic losses. It is clear from the figure that the business interruption plays the most important role, with about 80 % of *EL*. By checking both Figure 16 and Figure 17, it can be noticed that scenario #15, even though generates the biggest *EL*, equal to 11.6 million euros, the corresponding seismic damage mean annual frequency is rather small, while scenario #1 has economic losses of 10.8 million euros with the highest annual frequency. Therefore, it is important in this case to pay particular attention to damage scenario 1 and 2 in order to improve the seismic emergency plan of the nitric plant.

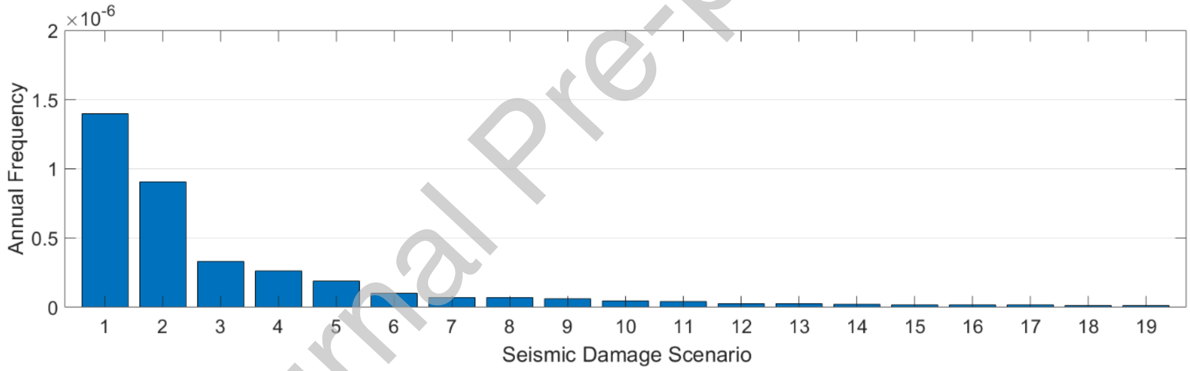

Figure 16 - Mean annual frequency of the most probable seismic damage scenarios.

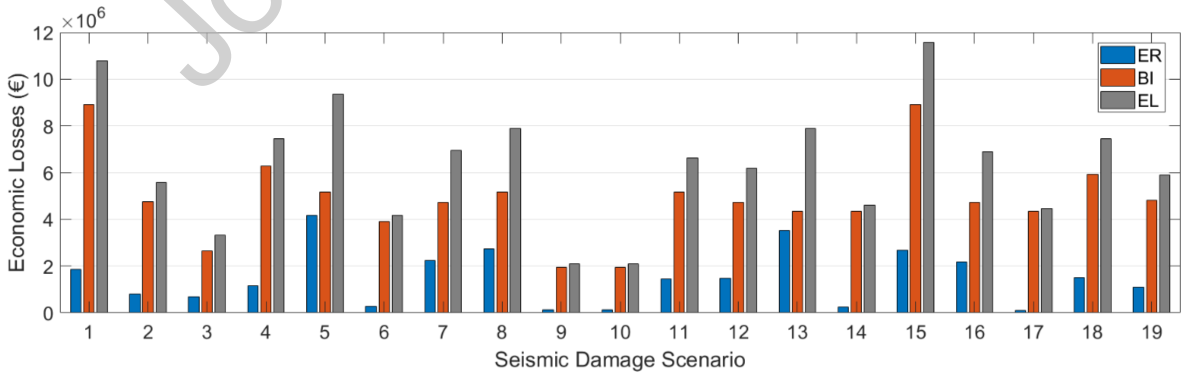

Figure 17 - Economic losses for seismic damage scenarios.

Figure 18 shows the recovery functions for the seismic damaged scenario #1 and #3 respectively. In scenario #1, E-21 and E-24 are damaged so the operational capacity at t_d drops to 0. The first recovery in operational capacity occurs at a time $t_c=T_{CR24}=170\ d$, time when E-24 is reconstructed and plant capacity increases to 40 % as the PF2 is back functional state. The total recovery time for this scenario corresponds to a time $t_r=T_{CR21}=180\ d$, time when E-21 is reconstructed and the plant operates with full capacity. This scenario has a resilience loss of 97.2 % which means it is very low resilient (R=2.8 %). This two equipment, E-21 and E-24 are very crucial for plant. In scenario 3, E-24 fails, so PF2 shuts down and plant capacity drops to 60 %. The full recovery time for this scenario is $t_r=T_{CR24}=170\ d$ leading to a resilience loss of 37.6 %. Seismic damage scenario #1 is the worst one as it has the biggest probability of occurrence and a very low resilience (R=2.8 %) so intervention need to be made to reduce the probability of failure or to increase it resilience.

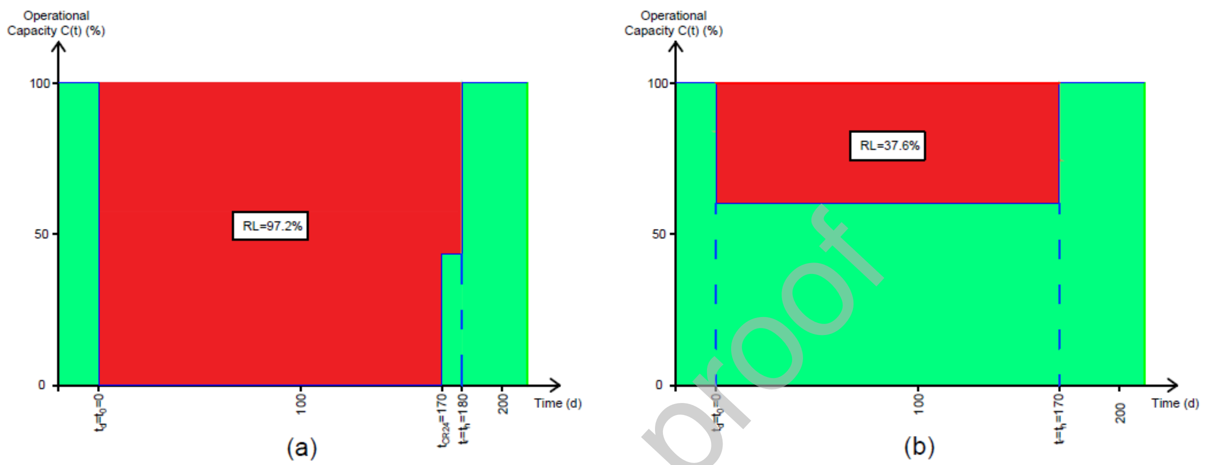

Figure 18 – Operational Capacity curve for most probable damage scenario: (a) scenario #1; (b) scenario #3.

It is important to know that the biggest economic losses are related to *BI* in order to set priorities in seismic emergency planning and to search different possible solutions to reduce these losses, such as adding more redundant units or proposing faster recovery strategies.

4. CONCLUSIONS

In this paper a novel methodology to estimate process plants resilience is proposed. The method, which is based on actual plant architecture, provides, for given damage scenarios, an estimate of the economic losses and business interruption costs, along with the time length of the capacity recovery phase. The proposed approach can incorporate either deterministic or probabilistic damage scenarios, representing a useful making decision tool for plant owners, facility planners and emergency managers in the process industry, in case of pure technological or Na-Tech events. In this respect, it contributes to fill the gap in the resilience calculation of process plants that during the last years seems to have not received the due attention.

Economic calculations, such as equipment reconstruction cost (direct losses) and business interruption (indirect losses) are integrated in methodology which can be useful even for insurance companies.

Concepts like Capacity Block Diagrams and Overall Reconstruction Activities Network, have been profitably used to determine the capacity loss and the recovery function of a process plant, which in turn allow to quantify direct (reconstruction costs) and indirect (business interruption) economic losses. The application of the method to a Nitric Acid plant in case of a seismic event, showed its usefulness and full potentiality.

Even though, domino scenarios have not considered and thus only units directly damaged by the earthquake have been considered, the method allowed to quantify for each scenario vector the indirect and direct costs loss, identifying the most critical components both under seismic and resilience point of view. In particular, the storage tanks of Nitric Acid (E-21) represents the most vulnerable element with the lowest resilience (40 %) and the highest mean annual frequency of occurrence of damage (1.39E-06). Moreover, this is the unit which corresponds to a particularly high *BI* (> 6 million €). The electric station (E-32) is equally critical even though with a higher resilience (50 %) and lower *BI* (< 5 million €). The seismic scenarios in which they are involved are #1, #2 and #3, where scenario #1 corresponds to the highest *BI* losses along with scenario #15. However, the mean annual frequency of occurrence of this latter rather low (< 1E-08) and thus can be considered negligible. It is important that decision makers and emergency planners consider seismic damage scenarios #1, #2 and #3 and to decide whether any actions are needed to be performed in order to reduce the seismic risk or to increase resilience.

The proposed method has been formulated under the hypothesis that a damaged component would be entirely reconstructed after being damaged. Moreover, the recovery capacity and time have been considered as deterministic. The extension to full probabilistic formulation and consideration of more damage limit states, will be the object of further studies.

To the best of the authors' knowledge, this is the first attempt to rationalize and quantify the concept of resilience for industry activities and in particular for process plants, which represents one of the most diffused and vulnerable type of plants, especially against Na-Tech events.

ACKNOWLEDGMENT

This project has received funding from the European Union's Horizon 2020 research and innovation programme under the Marie Sklodowska-Curie grant agreement No 721816.

REFERENCES

[1] Campedel M. Analysis of Major Industrial Accidents Triggered by Natural Events Reported in the Principal Available Chemical Accident Data- bases. European Union Joint Research Center, Institute for the Protection and Security of the Citizen, Ispra, Italy, 2008; Report No. EUR 23391 EN.

[2] Krausmann E, Cozzani V, Salzano E, Renni E. Industrial Accidents Triggered by Natural Hazards: An Emerging Risk Issue. Natural Hazards and Earth Systems 2011; Vol. 11, No. 3, pp. 921–929.

[3] Krausmann E, Cruz AM, Salzano E. Natech Risk Assessment and Management. Elsevier, 2017, Amsterdam, The Netherlands.

[4] Caputo AC, Giannini R, Paolacci F. Quantitative Seismic Risk Assessment of Process Plants. State of the Art Review and Directions for Future Research. ASME Paper No. PVP2015-45374, 2015.

[5] Caputo A C, Paolacci F, Bursi OS, Giannini R. Problems and perspectives in seismic QRA of chemical process plants for decision making. Submitted to Journal of Pressure Vessel and Technology. 2019; Volume 141 | Issue 1, DOI: 10.1115/1.4040804.

[6] Antonioni A, Spadoni G, Cozzani V. A methodology for the Quantitative Risk Assessment of Major Accidents Triggered by Seismic Events. Journal of of Hazardous Materials, 2007; Vol. 147, pp. 48-59.

[7] Antonioni G, Bonvicini S, Spadoni G, Cozzani V. Development of a Framework for the Risk Assessment of Na- Tech Accidental Events. Reliability Engineering and Systems Safety, 2009; Vol. 94, N. 9, pp. 1442-1450.

[8] Alessandri S, Caputo AC, Corritore D, Giannini R, Paolacci F, Phan HN. Probabilistic risk analysis of process plants under seismic loading based on Monte Carlo simulations. J Loss Prev Process Ind 2018;53:136–48. doi:10.1016/j.jlp.2017.12.013.

[9] Busini V, Marzo E, Callioni A, Rota R. Definition of a Short-cut Methodology for Assessing Earthquake-related Na-Tech Risk. Journal of Hazardous Materials, 2011; Vol. 192, pp. 329-339.

[10] Caputo AC. A model for Probabilistic Seismic Risk Assessment of Process Plants. Proc. ASME 2016 Pressure Vessels & Piping Conference PVP2016 July 17-21, Vancouver, British Columbia, Canada, Paper No. PVP2016-63280.

[11] Girgin S and Krausmann E. RAPID-N: Rapid Natech Risk Assessment and Mapping Framework. Journal of Loss Prevention in the Process Industries, 2013;Vol. 26, pp. 949-960.

[12] Naderpour M and Khakzad N. Texas LPG fire: Domino effects triggered by natural hazards. Process Safety and Environmental Protection, 2018; Vol. 116, 354-364.

[13] Bhamra R, Dani S, Burnard K. Resilience: The Concept, a Literature Review and Future Directions. International Journal of Production Research, 2011; Vol. 49, N.18, pp. 5375-5393.

[14] Hosseini S, Barker K, Ramirez-Marquez JE. A Review of Definitions and Measures of System Resilience. Reliability Engineering and System Safety, 2016; 145, pp. 47-61.

[15] Woods DW. Four concepts for resilience and the implications for the future of resilience engineering. Reliability Engineering and System Safety, 2015; Vol. 141, pp. 5-9.

[16] Hollnagel E, Woods DD, Leveson N. Resilience Engineering: Concepts and Precepts. Aldershot, UK: Ashgate Press,2006.

[17] Sheffi Y. The Resilient Enterprise: Overcoming Vulnerability for Competitive Advantage. The MIT Press, Cambridge, MA,2007.

[18] Rigaud E and Guarnieri F. Proposition of a Conceptual and a Methodological Modelling Framework for Resilience Engineering. Proc. 2nd Symp. on Resilience Engineering, Nov 2006, Juan-les-Pins, France.

[19] Lundberg J and Johansson BJE. Systemic resilience model. Reliability Engineering and System Safety, 2015; Vol. 141, pp. 22-32.

[20] Barker K, Ramirez-Marquez JE, Rocco CM. Resilience-Based Network Component Importance Measures. Reliability Engineering and System Safety, 2013;117, pp. 89-97.

[21] Cai B, Xie M, Liu Y, Liu Y, Feng Q. Availability-based engineering resilience metric and its corresponding evaluation methodology. Reliability Engineering and System Safety, 2018; 172, pp. 216-224.

[22] Henry D and Ramirez-Marquez JE. Generic Metrics and Quantitative Approaches for System Resilience as a Function of Time. Reliability Engineering and System Safety, 2012; 99, pp. 114-122.

[23] Francis R and Bekera B. A metric and Frameworks for Resilience Analysis of Engineered and Infrastructure Systems. Reliability Engineering and System Safety, 2014;121, pp. 90-103.

[24] Vugrin DE, Warren DE, Ehlen MA, Camphouse RC. A framework for assessing the resilience of infrastructure and economic systems, in Gopalakrishnan, K., Peeta, S., (Eds.). Sustainable and resilient critical infrastructure systems, 2010; Springer, Berlin.

[25] Annarelli A and Nonino F. Strategic and operational management of organizational resilience: Current state of research and future directions. Omega, 2016; Vol. 62, pp. 1-18.

[26] Burnard K and Bhamra R. Organisational Resilience: Development of a Conceptual Framework for Organisational Response. Int. J. of Prod. Res., 2011;49, No. 18, pp. 5581-5599.

[27] Bellamy LJ, Chambon M, van Guldener V. Getting resilience into safety programs using simple tools. A research background and practical implementation. Reliability Engineering and System Safety 172, 2018; pp. 171-184.

[28] Gunasekaran A, Rai BK, Griffin M. Resilience and competitiveness of small and medium size enterprises: An empirical research. International Journal of Production Research, 2011; Vol. 49, N. 18, pp. 5489-5509.

[29] Kamalahmadi M and Mellat Parast M. A Review of the Literature on the Principles of Enterprise and Supply Chain Resilience: Major Findings and Directions for Future Research. International Journal of Production Research, 2016; 171, pp. 116-133.

[30] Punter A, Coburn A, Ralph D, Tuveson M, Ruffle S, Bowman G. Evolving Risk Framework: Modeling Resilient Business Systems as Interconnected Networks. Proc. of ‘Think Outside the Risk’, Aon Benfield Hazards Conference, 22-24 September, 2013, Gold Coast, Australia.

[31] Sullivan-Taylor B and Branicki L. Creating resilient SMEs: why one size might not fit all. International Journal of Production Economics, 2011; Vol. 49, N. 18, pp. 5565-5579.

[32] Cimellaro GP and Martinelli D. Modelling Economic Dimension of Community Resilience. in Cimellaro, G.P. et al. (Eds.) Computational methods, Seismic Protection, Hybrid Testing and Resilience in Earthquake Engineering, 2015, pp. 185-202.

[33] Rose A and Krausmann E. An Economic Framework for the Development of a Resilience Index for Business Recovery. International Journal of Disaster Risk Reduction, 2013; 5, pp. 73-83.

[34] Broccardo M, Galanis P, Esposito S, Stodjanovic B. Probabilistic Resilience Assessment of Civil Systems: Analysis and Validity of the PEER Framework. in Podofillini et al., (Eds.) Safety and Reliability of Complex Engineered Systems, Taylor & Francis, London, 2015, pp. 331-339.

[35] Caverzan A and Solomos G. Review on Resilience in Literature and Standards for Critical Built-infrastructure, European Commission Internal Report,2014.

[36] Cimellaro GP. Urban Resilience for Emergency Response and Recovery. Fundamental Concepts and Applications. Springer, Berlin, 2016.

[37] Cimellaro G, Reinhorn AM, Bruneau M. Framework for Analytical Quantification of Disaster Resilience. Engineering Structures, 2010; Vol. 32, No. 11, pp. 3639–3649.

[38] Cimellaro GP, Bruneau M, Reinhorrn A. Quantification of Seismic Resilience. Proc 8th U.S. National Conf. on Earthquake Engineering, San Francisco, April 18-22, 2006, California, USA.

[39] Cimellaro GP, Reinhorn AM, Bruneau M. Seismic Resilience of a Hospital System. Struct. and Infrastr. Engineering, 2010; 6(1-2), pp. 127-144.

[40] Cimellaro GP, Renschler C, Bruneau M. Introduction to Resilience-Based Design (RBD), in Cimellaro, G.P. et al. (Eds.) Computational methods, Seismic Protection, Hybrid Testing and Resilience in Earthquake Engineering, 2015, pp. 151-183.

[41] Shafieezadeh A and Ivey Burden L. Scenario-Based Resilience Assessment Framework for Critical Infrastructure Systems: Case Study for Seismic Resilience of Seaports. Reliability Engineering and System Safety, 2014; 132, pp. 207-219.

[42] Tsionis G. Seismic Resilience: Concept, Metrics and Integration with other Hazards. European Commission, EUR 27038 EN – Joint Research Centre – Institute for the Protection and Security of the Citizen, 2014, ISBN 978-92-79-44723-5.

[43] Ramirez-Marquez JE, Rocco CM, Barker K, Moronta J. Quantifying the resilience of community structures in networks. Reliability Eng. and Syst. Safety, 2018; 169, pp. 466-474.
[44] Vargas VN and Ehlen MA. REAcct: a Scenario Analysis Tool for Rapidly Estimating Economic Impacts of Major Natural and Man-Made Hazards. Environment Systems and Decisions, 2013, 33, pp. 76-88.
[45] Hofer L, Zanini MA, Faleschini F, Pellegrino C. Profitability analysis for assessing the optimal seismic retrofit strategy of industrial productive processes with business interruption consequences, Journal of Structural Engineering, 2018, Vol. 144, No. 2, paper 04017205, pp. 1-13.
[46] Barabadi A and Ayele YZ. Post-disaster, infrastructure recovery: Prediction of recovery rate using historical data. Reliability Engineering and System Safety, 2018; 169, pp. 209-223.
[47] Barker K and Baroud H. Proportional Hazards Models of Infrastructure System Recovery. Reliability Eng. and Syst. Safety, 2014; 124, pp. 201-206.
[48] Cagno E, De Ambroggi M, Grande O, Trucco P. Risk Analysis of Underground Infrastructures in Urban Areas. Reliability Engineering and System Safety, 2011; 96, pp. 139-148.
[49] Conrad SH, LeClaire RJ, O’Reilly GP, Uzunalioglu H. Critical National Infrastructure Reliability Modeling and Analysis. Bell Labs Tech. J.l, 11(3), 2006, pp. 57–71.
[50] Filippini R and Silva A. A Modeling Framework for the Resilience Analysis of Networked Systems-of-Systems Based on Functional Dependencies. Reliability Engineering and System Safety, 2014; 125, pp. 82-91.
[51] Nan C and Sansavini G. A quantitative method for assessing resilience of interdependent infrastructures. Reliability Eng. and Syst. Safety, 2017; 157, pp. 35-53.
[52] Nguyen T, Cai X, Ouyang Y, Housh M. Modeling Infrastructure Interdependencies, Resiliency and Sustainability. International Journal of Critical Infrastructures, 2016; Vol. 12, N.1-2, pp 4-36.
[53] Ouyang M. Review on modeling and simulation of interdependent critical infrastructure systems. Reliability Engineering and System Safety, 2014; 121, pp. 43-60.
[54] Trucco P, Cagno E, De Ambroggi M. Dynamic Functional Modelling of Vulnerability and Interoperability of Critical Infrastructures. Reliability Engineering and System Safety, 2012; 105, pp. 51-63.
[55] Zhang X, Mahadevan S, Sankararaman S, Goebel K. Resilience-based network design under uncertainty. Reliability Eng. and Syst. Safety, 2018; 169, pp. 364-379.
[56] Baroud H and Barker K. A Bayesian kernel approach to modeling resilience-based network component importance. Reliability Engineering and System Safety, 2018; 170, pp. 10-19.
[57] Pettit TJ, Fiksel J, Croxton KL. Ensuring Supply chain resilience: Development of a conceptual framework. Journal of Business Logistics, 2013; Vol. 31, No. 1, 1-21.
[58] Pettit TJ, Croxton KL, Fiksel J. Ensuring Supply chain resilience: Development and implementation of an assessment tool. Journal of Business Logistics, 2013; Vol. 34, No. 1, 46-76.
[59] Brusset X and Teller C. Supply chain capabilities, risk and resilience. International Journal of Production Economics, 2017; Vol. 184, 59-68.
[60] Ivanov D, Dolgui A, Sokolov B, Ivanova M. Literature review on disruption recovery in the supply chain. International Journal of Production Research, 2017; Vol. 55, No. 20, pp. 6158-6174.
[61] Dinh LTT, Pasman H, Gao X, Mannan MS. Resilience Engineering of Industrial Processes: Principles and Contributing Factors. Journal of Loss Prevention in the Process Industry, 2012; 25, pp. 233-241.
[62] Eguchi H, Aoyama T, Seki K, O'Donovan D, Koshijima I. Organizational structure on the resilience of production processes based on human factors in the chemical industry. Journal of Engineering Science and Technology, 2015; Special issue on SOMCHE 20014 & RSCE 2014 Conference, pp. 30-40.
[63] Oedewald P, Macchi L, Axelsson C, Eitrheim MHR. Intermediate report of MoReMO. Modelling Resilience for Maintenance and Outage. NKS-262, NKS Secretariat, Roskilde, Denmark, 2012, ISBN 978-87-7893-335-5.
[64] Rydzak F, Chlebus E, Shirali GA, Shekari M, Angali KA. Quantitative assessment of resilience safety culture using principal components analysis and numerical taxonomy: A case study in a petrochemical plant. Journal of Loss Prevention in the Process Industries, 2016; Vol. 40, pp. 277-284.

[65] Aven T. How some types of risk assessment can support resilience analysis and management. Reliability Engineering and System Safety, 2017; Vol. 167, pp. 536-543.
[66] Castillo-Borja F, Vazquez-Roman R, Quiroz-Perez E, Diaz-Ovalle C, Mannan MS. A Resilience Index for Process Safety Analysis. Journal of Loss Prevention in the Process Industries, 2018; Vol. 50, pp. 184-189.
[67] Jain P, Rogers WJ, Pasman HJ, Keim KK, Mannan MS. A resilience-based integrated process systems hazard analyisis (RIPSHA) approach: Plant system layer. Process Safety and Environmental Protection, 2018; Vol. 116, 92-105
[68] Jain P, Pasman HJ, Waldram S, Pistikopoulos EN. Process resilience analysis framework (PRAF): A systems approach for improved risk and safety management. Journal of Loss Prevention in the Process Industries, 2018; Vol. 53, pp. 61-73.
[69] Jain P, Mentzer R, Mannan SM. Resilience metrics for improved process-risk decision making: Survey, analysis and application. Safety Science, 2018; Vol. 108, pp. 13-28.
[70] Rydzak F, Magnuszewski P, Sendzimir J, Chlebus E. A concept of Resilience in Production Systems. Proc. 24th Int. Conf. of the System Dynamics Society, July 23-27, 2006; Nijmegen, The Netherlands, https://www.systemdynamics.org/ conferences/2006/proceed/.
[71] Rydzak F and Chlebus E. Application of Resilience Analysis in Production Systems – Bombardier Transportation Case Study. Proc. 25th International Conference of the System Dynamics Society, July 29-August 2, 2007, Massachusetts Institute of Technology, Cambridge, USA.
[72] Ganesan T and Elamvazuthi I. A multi-objective approach for resilience based plant design optimization. Quality Engineering, 2017; Vol. 29, No. 4, pp. 656-671.
[73] Tan RR, Aviso KB, Cayamanda, CD, Chiu ASF, Promentilla MAB, Ubando AT, Yu KDS. A Fuzzy Linear Programming Enterprise Input-Output Model for Optimal Crisis Operations in Industrial Complexes. International Journal of Production Economics, 2016; 181, Part B, pp. 410–418.
[74] Zio E and Ferrario E. A Framework for the System-of-Systems Analysis of the Risk for a Safety-Critical Plant Exposed to External Events. Environ. Syst. and Decisions, 2013; 114, pp. 114-125.
[75] Ferrario E and Zio E. Goal Tree Success tree-Dynamic Master Logic Diagram and Monte Carlo simulation for the safety and resilience assessment of a multistate system of systems. Engineering Structures, 2014; Vol. 59, pp. 411-433.
[76] Ferrario E and Zio E. Assessing Nuclear Power Plant Safety and Recovery from Earthquakes Using a System-of-Systems Approach, Reliability Engineering and System Safety, 2014; 125, pp. 103-116.
[77] Mebarki A, Jerez S, Prodhomme G, Reimeringer M. Natural Hazards, Vulnerability and Structural Resilience: Tsunamis and Industrial tanks. Geomatics, Natural Hazards and Risk, 2016; Vol. 7, suppl. 1, pp. 5-17.
[78] Yao H. The Modeling, Analysis and Control of Resilient Manufacturing Enterprises. Doctoral dissertation in Electrical and Computer Engineering. 2013, Paper 15., http://uknowledge.uky.edu/ece_etds/15.
[79] Caputo AC and Paolacci F. A method to estimate process plant resilience. Proc. ASME Pressure Vessel & Piping Conference 2017, July 16-20, 2017, Waikoloa, Hawaii, United States, Paper # PVP2017-65464.
[80] Cimellaro GP, Fumo C, Reinhorn AM, Bruneau M. Quantification of disaster resilience of health care facilities. Technical Report MCEER-09-0009, University at Buffalo, USA, 2009.
[81] Bruneau M, Chang SE, Eguchi RT, Lee GC, O'Rourke TD, Reinhorn AM, Shinozuka M, Tierney K, Wallace WA, von Winterfeldt D. A Framework to Quantitatively Assess and Enhance the Seismic Resilience of Communities. Earthquake Spectra, 2003; 19(4), pp. 733-752.
[82] Bocchini P and Frangopol DM. Resilience-Driven Disaster Management of Civil Infrastructures. Proc. Conf. on Computational Methods in Structural Dynamics and Earthquake Engineering, Corfu, Greece,2011.
[83] Vanhoucke M. Project Management with Dynamic Scheduling. Berlin, Heidelberg: Springer Berlin Heidelberg; 2012; doi: 10.1007/978-3-642-25175-7.

[84] Cornell A. Engineering Seismic Risk Analysis. Bull. of the Seismological Society of America October 1968, Vol. 58, N. 5, pp. 1583-1606.
[85] Phan HN, Paolacci F, Alessandri S, Enhanced seismic fragility analysis of unanchored steel storage tanks accounting for uncertain modeling parameters, submitted to Journal of Pressure Vessel and Technology, 2019; Volume 141 | Issue 1, DOI: 10.115/1.4039635
[86] Salzano E, Iervolino I, Fabbrocino G. Seismic Risk of Atmospheric Storage Tanks in the Framework of Quantitative Risk Analysis. J. of Loss Prev. in Proc. Ind., 2003; 16, pp. 403-409.
[87] PEC (2017). Deliverable D4.1 - Definition of the structural models and seismic fragility analysis techniques available for the specific case study. PEC Project: Post-Emergency, Multi-Hazard Health Risk Assessment in Chemical Disasters, 2017.
[88] Hazus – MH 2.1 Technical manual, Earthquake model, Multi-hazard Loss Estimation Methodology.
[89] Phan HN, Paolacci F, Bursi OS, Tondini N. Seismic fragility analyses of elevated steel storage tanks supported by reinforced concrete columns. Journal of Loss Prevention in the Process Industries, 2017; 47; 57-65, DOI: 10.1016/j.jlp.2017.02.017
[90] Zentner I, Gündel M, Bonfils N. Fragility analysis methods: Review of existing approaches and application. Nuclear Engineering and Design, 2017; 323, 245–258
[91] D'Amico M and Buratti N. Observational Seismic Fragility Curves for Steel Cylindrical Tanks. ASME. J. Pressure Vessel Technol. 2018; 141(1), DOI:10.1115/1.4040137.
[92] Paolacci F, Corritore D, Caputo AC, Burso O, Kalemi B, A probabilistic approach for the assessment of LOC events in steel storage tanks under seismic loading, ASME 2018 Pressure Vessels and Piping Conference, PVP 2018, Prague, Czech Republic, 15 July 2018 through 20 July 2018, Code 141606, DOI:10.1115/PVP2018-84374
[93] Fabbrocino G, Iervolino I, Orlando F, Salzano E. Quantitative Risk Analysis of Oil Storage Facilities in Seismic Areas. J. of Hazardous materials, 2005; A123, pp. 61-69.
[94] Campedel M, Cozzani V, Garcia-Agreda A, Salzano E. Extending the Quantitative Assessment of Industrial Risks to Earthquake Effects. Risk Analysis, 2008; 28(5), pp.1231-1246.
[95] Finney DJ. Probit analysis. Cambridge University Press, Cambridge, UK, 1971.
[96] Rubinstein RY and Kroese DP. Simulation and the Monte Carlo Method. 2nd ed., J.Wiley and Sons, 2008.
[97] Ray MS and Johnston DW. Chemical engineering design project: A case study approach. Topics in chemical engineering Volume 6, 1989.
[98] CEPCI Online, Chemical Engineering Plant Cost Index https://www.chemengonline.com/2018-cepci-updates-july-prelim-and-june-final/
[99] Vatavuk MW. Updating the CE cost plant index. Chemical Engineering www.CHE.com January 2012.
[100] Corritore D, Alessandri S, Giannini R, Paolacci F. PRIAMUS: A new tool for the probabilistic risk assessment with Monte Carlo simulations of Process Plants under Seismic Loading. ANIDIS Conference, Pistoia, 2017.